Neoplasia • Vol. 7, No. 3, March 2005, pp. 207–223 207

www.neoplasia.com

Bone Microenvironment Modulates Expression and Activity of Cathepsin B in Prostate Cancer[1]

Izabela Podgorski, Bruce E. Linebaugh*, Mansoureh Sameni*, Christopher Jedeszko*, Sunita Bhagat[†], Michael L. Cher[†,‡,§] and Bonnie F. Sloane*[,§]*

Departments of *Pharmacology, [†]Urology and [‡]Pathology, Wayne State University School of Medicine, Detroit, MI 48201, USA; [§]Barbara Ann Karmanos Cancer Institute, Detroit, MI 48201, USA

Abstract

Prostate cancers metastasize to bone leading to osteolysis. Here we assessed proteolysis of DQ-collagen I (a bone matrix protein) and, for comparison, DQ-collagen IV, by living human prostate carcinoma cells *in vitro*. Both collagens were degraded, and this degradation was reduced by inhibitors of matrix metallo, serine, and cysteine proteases. Because secretion of the cysteine protease cathepsin B is increased in human breast fibroblasts grown on collagen I gels, we analyzed cathepsin B levels and secretion in prostate cells grown on collagen I gels. Levels and secretion were increased only in DU145 cells—cells that expressed the highest baseline levels of cathepsin B. Secretion of cathepsin B was also elevated in DU145 cells grown *in vitro* on human bone fragments. We further investigated the effect of the bone microenvironment on cathepsin B expression and activity *in vivo* in a SCID-human model of prostate bone metastasis. High levels of cathepsin B protein and activity were found in DU145, PC3, and LNCaP bone tumors, although the PC3 and LNCaP cells had exhibited low cathepsin B expression *in vitro*. Our results suggest that tumor–stromal interactions in the context of the bone microenvironment can modulate the expression of the cysteine protease cathepsin B.

Neoplasia (2005) **7,** 207–223

Keywords: Cathepsin B, bone microenvironment, prostate cancer, osteolysis, tumor–stromal interactions.

Introduction

Metastasis to the bones is commonly observed in advanced prostate cancer. The interaction of tumor cells with the bone microenvironment may lead to a selective advantage for tumor growth in bones compared to tumor growth in other organ microenvironments. Successful tumor invasion requires degradation of extracellular matrices by multiple proteases, including matrix metalloproteases (MMPs), serine proteases [urokinase plasminogen activator (uPA), plasmin], aspartic proteases, and cysteine proteases, but the relative contribution of individual proteases is still debated. Proteolytic enzymes from all four classes have been shown to degrade extracellular matrix proteins and basement membrane *in vitro* [1–3]. *In vivo* studies reveal decreases in staining for extracellular matrix proteins at the invading edges of tumors, perhaps indicative of proteolytic degradation by tumor cells [4,5].

Several mechanisms appear to be associated with metastatic processes including interactions of tumor cells with surrounding stroma; interactions with extracellular matrix; release of cytokines, growth factors, and proteolytic enzymes; and altered cell attachment and proliferation. Interactions between cancer cells and the host environment are critical for successful tumor invasion. In prostate cancer, understanding the bone microenvironment is important for the assessment of the mechanisms of preferential metastasis to the bones. Within bones, there is a highly abundant and metabolically active bone marrow consisting of hematopoietic and mesenchymal stem cells, which give rise to blood cells, osteoclasts, osteoblasts, adipocytes, chondrocytes, and stromal cells. Bone-forming osteoblasts and bone-resorbing osteoclasts are of particular importance, as cancer cells use the normal bone remodeling machinery to successfully colonize the bone and subsequently degrade it [6]. The main organic component of bone is type I collagen, a protein implicated in the attachment and proliferation of various cancer cells in skeletal tissues [7,8]. The interactions of tumor and stromal cells with collagen I and other extracellular matrix proteins can alter their protease expression [9–11]. For example, we have previously shown that the growth of human breast fibroblasts in collagen I gels alters the expression of the cysteine protease cathepsin B, a process regulated by integrin binding to collagen I [12].

Abbreviations: MMP, matrix metalloprotease; uPA, urokinase plasminogen activator; SCID, severe combined immunodeficient; Z-Arg-Arg-NHMec, benzyloxy-carbonyl-arginyl-arginyl-aminomethylcoumarin; TRAP, tartrate-resistant acid phosphatase; TGF-β, transforming growth factor-β; PTHrP, parathyroid hormone–related protein

Address all correspondence to: Dr. Izabela Podgorski, Department of Pharmacology, Wayne State University School of Medicine, 540 East Canfield, Detroit, MI 48201. E-mail: ipodgors@med.wayne.edu

[1]This work was supported by DOD Award PC991261 and DOD Postdoctoral Fellowship PC030325. The Zeiss LSM-310 confocal microscope was supported, in part, by the National Institutes of Health NIEHS grant P30ES06639 and NCI grant P30CA22453.

Received 27 May 2004; Revised 28 July 2004; Accepted 6 August 2004.

DOI 10.1593/neo.04349

Increased expression of cathepsin B occurs at the invading edges of many tumors (i.e., the edges interacting with extracellular matrices) [13,14]. Altered expression and activity at the tumor–stromal interface suggest that this protease may be one key player in the events associated with tumor cell invasion. Cathepsin B has been shown to activate the serine protease pro-uPA to uPA [15,16], leading to the activation of serum-derived latent transforming growth factor [17]. Cathepsin B also increases MMP activity directly by activation of the proenzymes [18], and indirectly through degradation of tissue inhibitors of MMPs (TIMPs) [19]. A continuous interplay between prostate cancer cells and the bone microenvironment is a critical feature of bone metastasis. Here we demonstrate that osteolytic DU145 prostate carcinoma cells express high levels (message, protein, and activity) of cathepsin B, and that these levels are further increased by interaction with collagen I or the human bone. Interaction with the human bone leads to secretion of the active enzyme, suggesting the importance of tumor–stroma and tumor–host interactions in the regulation of cathepsin B in prostate cancer cells. The importance of the tumor–stroma interface and the impact of the metabolically rich bone microenvironment are further validated by *in vivo* studies using a SCID-human model of prostate cancer metastasis [20]. Upregulation of cathepsin B expression and activity in DU145, PC3, and LNCaP bone tumors are observed—a result consistent with an involvement of cathepsin B in prostate cancer metastasis to the bones.

Experimental

Materials

RPMI 1640, Dulbecco's modified Eagle's medium (DMEM), BGJ_B, MES (2-[*N*-morpholino] ethane-sulfonic acid), PIPES (piperazine-*N*′*N*′-bis[2-ethanesulfonic acid]), Hanks salt solution, sodium bicarbonate, antibiotics, dimethyl sulfoxide (DMSO), paraformaldehyde, the broad-spectrum cysteine protease inhibitor E-64, the serine protease inhibitor aprotinin, and other chemicals, unless otherwise stated, were obtained from Sigma (St. Louis, MO). Fetal bovine serum (FBS), trypsin–EDTA, collagenase, and Trizol reagent were obtained from Invitrogen (Carlsbad, CA). Vitrogen-100 collagen type I was from Cohesion Laboratories (Palo Alto, CA). The quenched fluorescent substrates, DQ-collagen I and DQ-collagen IV, and SlowFade antifade reagent were purchased from Molecular Probes (Eugene, OR). The fluorogenic substrate Z-Arg-Arg-NHMec and its cleavage product NH2Mec were purchased from Bachem (King of Prussia, PA). CA074 and its membrane-permeable derivative CA074Me were purchased from Peptides International (Louisville, KY). The broad-spectrum MMP inhibitor GM6001 was purchased from Chemicon (Temecula, CA). Rabbit antihuman cathepsin B antibodies were produced and characterized in our laboratory [21]. Fluorescein or Texas Red–conjugated donkey antirabbit IgG and normal donkey serum were obtained from Jackson ImmunoResearch (West Grove, PA). Horseradish peroxidase–labeled goat antirabbit IgG and microbicinchoninic acid (BCA) protein kit were purchased from Pierce (Rockford, IL). Western blotting detection kits were from Amersham Pharmacia Biotechnologies (Piscataway, NJ). *In situ* hybridization Renaissance TSA-Indirect detection kit was obtained from NEN Life Sciences (Boston, MA). The 25-mer 5′-biotin–labeled cathepsin B DNA oligonucleotides were synthesized by Integrated DNA Technologies, Inc. (Coralville, IA).

Cell Lines

Three human prostate carcinoma cell lines were purchased from American Type Culture Collection (ATCC; Manassas, VA): DU145, an androgen-independent osteolytic line derived from a brain metastasis [22]; PC3, an androgen-independent osteolytic line derived from a bone metastasis of a high-grade adenocarcinoma [23]; and LNCaP, an androgen-dependent, mixed-response (osteolytic/osteoblastic) cell line derived from a lymph node metastasis [24]. DU145 and PC3 cells were cultured in DMEM supplemented with 10% FBS and LNCaP cells were cultured in RPMI 1640 supplemented with 10% FBS according to ATCC guidelines. All cell cultures were maintained in a 37°C humidified incubator ventilated with 5% CO_2.

Proteolysis by Living Cells

Assays for proteolysis were performed accordingly to previously published procedures [25–27]. Briefly, glass coverslips were coated with 30 μl of 25 μg/ml quenched fluorescent substrates DQ-collagen IV mixed with Matrigel, or DQ-collagen I mixed with Vitrogen-100 bovine collagen I. The ratios of quenched fluorescent components to nonfluorescent components were identical for the collagen I and collagen IV experiments (1:40). Cells were seeded at a density of 50,000 cells per coverslip and cultured in serum-containing media indicated above for 40 to 44 hours. The degradation of the quenched fluorescent collagens due to the generation of fluorescent cleavage products was then observed by confocal microscopy on a Zeiss LSM 310 using a ×40 water immersion lens. For inhibitor studies, the following compounds were used: the selective cell-impermeable cathepsin B inhibitor, 5 μM CA074 [28,29]; the selective cell-permeable cathepsin B inhibitor, 5 μM CA074Me [30]; a broad-spectrum cysteine protease inhibitor, 10 μM E-64; a broad-spectrum MMP inhibitor, 25 μM GM6001; or an inhibitor of the plasminogen pathway, 2 μM aprotinin. Inhibitors were added to both the matrices and the media, and were replenished after 24 hours. All inhibitors were added in DMSO vehicle, and control cells were grown in the presence of vehicle alone.

Viability Assays

Cell viability under assay conditions was assessed using propidium iodide staining according to the manufacturer's protocol (Molecular Probes). Briefly, cells were grown on Matrigel-coated or collagen I–coated coverslips for 40 to 44 hours, washed 3× at 37°C with Tris buffer (100 mM Tris,

pH 7.4, 150 mM NaCl, 1 mM $CaCl_2$, 0.5 mM $MgCl_2$, and 0.1% Nonidet P-40), and stained with 3 μM propidium iodide nucleic acid stain in Tris buffer for 15 minutes. Cells were then washed 3× with Tris buffer and, after adding serum free media, observed with a Zeiss LSM 310 microscope with a 40× water immersion lens.

Quantification and Statistical Analysis

Fluorescence intensities in the absence and presence of various inhibitors were quantified from confocal fluorescent images using Image J Software (National Institutes of Health, Bethesda, MD). For the analysis of degradation of DQ-collagen IV by DU145 and PC3 cells, mean fluorescence was measured directly over the area of the spheroid as well as over the areas of pericellular fluorescence where cells were not present. This measurement was performed for multiple fields within a single image, and then normalized to the smallest area measured for each of the carcinoma cell lines (see footnote to Table 1). Because DU145 and PC3 cells do not form spheroids when grown on collagen I, and LNCaP cells do not form spheroids on either collagen, for those assays, we assessed mean fluorescence based on five arbitrary squares of defined area (22,500 Px^2) per field. Statistical significance was determined by a two-tailed *t*-test with assumed equal variance. $^*P \leq .05$ was considered statistically significant.

Cell Cultures on Collagen I Gels

Collagen I gels were prepared according to previously published procedures [12]. Prostate carcinoma cells (1×10^6 cells/dish) were seeded on uncoated or collagen I–coated (0.25 mg/cm^2) 100-mm^2 tissue culture dishes, grown for 60 hours, and then serum-starved for an additional 12 hours. Cells were harvested (at ~80% confluency) from collagen I gels using 0.1% collagenase at 37°C for 10 to 20 minutes. Cell pellets were washed in phosphate-buffered saline (PBS); resuspended in 250 mM sucrose, 25 mM MES, 1 mM EDTA, pH 6.5, and 0.1% Triton X-100 (SME buffer); lysed by sonication; and frozen at −80°C until used. DNA concentration was determined by the method of Downs and Wilfinger [31], and protein was determined using MicroBCA protein assay kit. Conditioned media were passed through Millipore 100K concentrators (Burlington, MA) at 150g to remove large collagen fragments and were concentrated using Millipore 10K concentrators.

Cell Cultures on Human Bone Fragments

For cell bone cocultures, human male fetal femurs (16–19 weeks gestation) were obtained from Advanced Bioscience Resources (Alameda, CA). The bones were cut longitudinally and then transversely into six fragments and maintained in a 24-well plate (two pieces per well) in serum-free BGJ_B medium for 24 hours. After equilibration, prostate

Table 1. Protease Inhibitors Reduce Collagen Degradation by Prostate Carcinoma Cells.

	DQ-Collagen IV		DQ-Collagen I	
	Mean Fluorescence*	Area†	Relative Fluorescence‡	Mean Fluorescence*,§
DU145				
Control	41 ± 10	45,724	18	26 ± 6
CA074/CA074Me	2 ± 1¶	19,756#	2	18 ± 8
E-64	2 ± 1¶	24,612	2	14 ± 5
GM6001	2 ± 2¶	24,015	2	9 ± 0#,¶
Aprotinin	4 ± 3¶	32,695	2	16 ± 2
PC3				
Control	34 ± 12	101,537	17	24 ± 6
CA074/CA074Me	3 ± 3¶	65,665	2	7 ± 5#,¶
E-64	3 ± 2¶	54,992	2	14 ± 3
GM6001	2 ± 1¶	54,187	2	11 ± 6
Aprotinin	5 ± 5¶	49,997#	2	14 ± 8
LNCaP				
Control	6 ± 1	22,500§		13 ± 3
CA074/CA074Me	5 ± 2¶	22,500§		5 ± 5
E-64	6 ± 0*,¶	22,500§		6 ± 2*,¶
GM6001	3 ± 0*,¶	22,500§		3 ± 1*,¶
Aprotinin	4 ± 0*,¶	22,500§		6 ± 2*,¶

Degradation was assessed as fluorescent degradation products present within the areas specified for the three prostate carcinoma cell lines grown either on Matrigel mixed with DQ-collagen IV or bovine type I collagen mixed with DQ-collagen I (see Experimental section for a more detailed description). Controls contained the diluent DMSO at a concentration of 0.1%; the final concentrations of the inhibitors were 5 μM CA074 + 5 μM CA074Me, 10 μM E-64, 25 μM GM6001, or 2 μM aprotinin.

*Mean fluorescence ± SD is the sum of the gray scale value for the pixels measured directly within a single image and is expressed in arbitrary units measured using Image J Software.

† Area (in Px^2) represents the total area over which the mean fluorescence was assessed (i.e., the area of the spheroid + areas of pericellular fluorescence in which cells were not present).

‡ Relative fluorescence was calculated for those cells that grow as spheroids in order to normalize the values of fluorescence to the smallest area measured for each of the carcinoma cell lines.

§ Five randomly chosen areas of 22,500 Px^2 in each field were used to calculate mean fluorescence.

¶ Indicates $P < .05$ compared to the control for each cell line.

The area used for normalization.

carcinoma cells were seeded on bone fragments (marrow side up) in 500 μl of BGJ_B media containing 1% horse serum (1×10^5 cells/well) for 48 hours. Additional wells, containing prostate carcinoma cells alone or bone fragments alone, were also cultured in 500 μl of BGJ_B media containing 1% horse serum. After 48 hours, conditioned media were collected, wells were washed twice with "real-time assay buffer" (Hanks balanced salt solution lacking sodium bicarbonate and containing 0.6 mM $CaCl_2$, 0.6 mM $MgCl_2$, 25 mM PIPES, 2 mM L-cysteine, and 10 mM D-glucose, adjusted to pH 7.0), and 400 μl of "real-time assay buffer" was added for analysis of secretion of active cathepsin B from the cocultures [32]. Following assay, the wells were washed twice with PBS and the contents were homogenized in SME buffer for analysis of activity in total cell lysates.

Northern Blot Analysis

Total cellular RNA from prostate carcinoma cells grown on plastic, or collagen I gels were extracted using Trizol reagent according to the manufacturer's instructions. Electrophoresis (20 μg/lane) was performed on an 0.8% agarose formaldehyde-denaturing gel. Gels were then transferred using Turboblotter, UV-crosslinked, hybridized, and analyzed according to previously described procedures [12]. Glyceraldehyde-3-phosphate dehydrogenase (*GAPDH*) was used as a loading control.

Sodium Dodecyl Sulfate Polyacrylamide Gel Electrophoresis and Immunoblotting

Samples of lysates, tissue extracts, or conditioned media were electrophoresed on 12% SDS gels. For collagen I studies, samples were loaded based on their DNA concentrations, whereas human bone samples and tissue extracts were loaded based on their protein/DNA ratios to account for the effect of bone microenvironment on cell size. All gels were transferred to nitrocellulose membranes and immunoblotted using 3 μg/ml primary rabbit antihuman cathepsin B antibody [21] and horseradish peroxidase–labeled secondary goat antirabbit IgG (1:12,000). Quantitation and analysis of bands were performed using a Luminescent Image Analyzer LAS-1000 Plus (Fujifilm, Stamford, CT) and expressed as arbitrary units (AU) per square millimeter.

Immunofluorescent Staining of Prostate Carcinoma Cells Grown on Plastic and Collagen I Gels

Prostate carcinoma cells were grown on uncoated or collagen I–coated coverslips for 48 to 72 hours (~80% confluence). Intracellular cathepsin B was immunolocalized in 0.1% saponin-permeabilized cells according to our previously published procedures [25]. The primary antibody was rabbit antihuman liver cathepsin B (5 μg/ml) [21]. Controls were run in the absence of primary antibody. Secondary antibodies were fluorescein-conjugated donkey antirabbit IgG. Coverslips were mounted upside down on glass slides using SlowFade antifade reagent and observed on a Zeiss LSM 310 confocal microscope.

Assays for Cathepsin B Activity in Cell Lysates and Conditioned Media

Cathepsin B activity was determined by our previously published procedures [32,33]. In cell lysates, cathepsin B was preincubated with 10 mM DTT and 50 mM EDTA, pH 5.5, for 15 minutes at 37°C. Activity was then assayed by adding the fluorometric substrate Z-Arg-Arg-NHMec (final concentration, 100 μM) in "real-time assay buffer" without L-cysteine and D-glucose. The activity of latent or procathepsin B in conditioned media was assayed following activation with pepsin as has been described [12]. Cathepsin B activity produced pericellularly by live cells (i.e., in real time) was assayed as previously described [32]. Briefly, wells containing cells alone, bone fragments alone, or cells and bone together were incubated with "real-time assay buffer" containing 100 μM Z-Arg-Arg-NHMec at 37°C. The progress of the reaction was monitored every minute for a period of 30 minutes on a Fluoroskan II microplate reader. Similar assays were performed with prostate carcinoma cells grown on collagen I gels. Results of all activity assays are expressed as picomoles of NH_2Mec formed per minute per cell unit. Cell units were calculated as the protein/DNA ratio (mg protein/μg DNA) to account for the effect of the metabolically active bone microenvironment on cell size. Statistical significance was determined by a two-tailed *t*-test with assumed equal variance and $P \leq .05$ was considered statistically significant.

Tissue Implantation and Establishment of Human Bone Tumors

Five-week–old male homozygous ICRSC-M *scid* mice were purchased from Taconic Farms (Germantown, NY) and were allowed to acclimate in their housing for 1 week. Mice were maintained under aseptic conditions according to the NIH guidelines as found in the "Guidelines for the Care and Use of Experimental Animals." All of the experimental protocols were approved by the Animal Investigation Committee at Wayne State University. Implantation with human bone fragments and tumor cell injections were performed under isoflurane inhalational anesthesia according to previously published procedures [20]. Briefly, fetal bones were cut longitudinally and then transversely into six fragments, and single bone fragments were implanted into both flanks of the mouse with the opened marrow cavity placed facing the abdomen. Following a 4-week engraftment, SCID-human mice were injected intraosseously (directly into the marrow) with prostate carcinoma cells (DU145, PC3, or LNCaP; three animals per group; two injection sites per animal). On the day of injection, prostate carcinoma cells were trypsinized, washed in PBS, and resuspended in PBS (5×10^5 cells/50 μl). Prostate carcinoma cells were injected into the marrow side of the implanted bone using a 27-gauge needle. Control groups obtained subcutaneous injections of prostate carcinoma cell lines (1×10^6 cells/50 μl PBS) into both flanks of the mouse (three mice per group). Mice were euthanized by cervical dislocation before resulting tumors were removed. In the initial experiment, bone tumors were collected when easily palpable through the skin (5–7 weeks after injection). In the two follow-up studies, tumors were removed 2,4, and 6 weeks after injection. Subcutaneous

tumors were removed when palpable through the skin (6–7 weeks after injection).

Preparation of Tissue Extracts for Immunoblots and Activity Assays

All harvested tumors were immediately divided into two equal parts. One part was fixed and embedded for sectioning (see Immunohistochemistry and *In Situ* Hybridization of Human Bone Tumors section), and the other was homogenized in 500 μl of SME buffer. Resulting extracts were centrifuged at 3000 rpm for 10 minutes, and supernatants were collected and frozen at −80°C. Immunoblotting and activity assays were performed as described above for cell lysates.

Immunohistochemistry and In Situ Hybridization of Human Bone Tumors

Part of each tumor was fixed overnight in 4% paraformaldehyde, decalcified in 10% EDTA for 2 weeks, and paraffin-embedded. Serial sections (4 μm) were cut, deparaffinized, and rehydrated. Hematoxylin and eosin (H&E) staining was performed to examine histologic changes. Immunofluorescent staining of adjacent sections of each tumor was performed using a cathepsin B antibody (1:400) purified in our laboratory [21]. Controls were run in the absence of primary antibody. Secondary antibodies were fluorescein-conjugated donkey antirabbit IgG. For *in situ* hybridization, deparaffinized tissues were treated with proteinase K (15 μg/ml) for 30 minutes at 37°C, fixed in 4% paraformaldehyde, and prehybridized in buffer containing 25% formamide, 1 μg/μl yeast, 2× SSC (0.3 M NaCl, 0.03 M sodium citrate), and 0.2 μg/μl BSA for 2 hours at 42°C. Four antisense and two sense cathepsin B oligonucleotides were used in the hybridization protocol. For antisense hybridization, four probes were combined (5′-/5Bio/GTT GGA AGC CGG ATC CTA GAT CCA C-3′; 5′-/5Bio/CCT CTT CAA GTA GCT CAT GTC CAC G-3′; 5′-/5Bio/AGG ATA GCC ACC ATT ACA GCC GTC C-3′; and 5′-/5Bio/CTC ACA TGG CCT GTC TGC ACT GTA A-3′), and for sense hybridization, two combined sense probes were used (5′-/5Bio/CGT GGA CAT GAG CTA CTT GAA GAG G-3′; and 5′-/5Bio/TTA CAG TGC AGA CAG GCC ATG TGA G-3′). Serial slides were incubated with probe-containing (5 ng/μl) hybridization buffer overnight at 42°C. Mock hybridization was performed as a control with each experiment. Detection of the hybridization signal was based on TSA-Indirect protocol for *in situ* hybridization. Immunofluorescence results of immunohistochemistry and *in situ* hybridization were observed on a Zeiss LSM 310 confocal microscope.

Results

Imaging Degradation of DQ-Collagen IV and DQ-Collagen I by Living Prostate Cancer Cells

A novel confocal assay has been developed in our laboratory to examine proteolysis by living cells [25–27]. In the present study, we used this assay to examine the ability of prostate carcinoma cells to degrade quenched fluorescent derivatives of collagen IV (basement membrane) and collagen I (organic matrix of the bone). We plated DU145, PC3, and LNCaP cells on DQ-collagen IV mixed with Matrigel (Figure 1) or DQ-collagen I mixed with collagen I (Figure 2), and visualized the fluorescence degradation products at 48 hours after plating. Phase images of the cells on Matrigel (Figure 1) revealed that DU145 cells formed tight spheroids, PC3 cells formed loose spheroids, and LNCaP cells grew as clusters or strings of cells. Degradation of the DQ-collagen IV could be observed as green fluorescence, with the DU145 cells exhibiting greater degradation than either the PC3 or LNCaP cells. Fluorescent cleavage products of DQ-collagen IV were found both intracellularly and pericellularly. On collagen I, the three prostate carcinoma cells grew as monolayers (Figure 2). Degradation products of DQ-collagen I were less intense (Figure 2) than observed for DQ-collagen IV (Figure 1), indicating that DQ-collagen I was digested to a lesser extent by the prostate carcinoma cells. This is consistent with our studies utilizing purified components, in which collagen IV was more readily degraded than collagen type I (data not shown). In the present study, DQ-collagen I degradation products were mainly pericellular (Figure 2).

To assess the involvement of proteases in the degradation of the two collagens, we used inhibitors of different protease classes. Representative images are illustrated in Figures 1 and 2, and the quantified results for each treatment are summarized in Table 1. As we had established that cathepsin B participates in the degradation of DQ-collagen IV by human breast [25,27] and colon [27] cancer cells, we tested the effects of incubation with the highly selective cell-impermeant cathepsin B inhibitor CA074 [28] in combination with its cell-permeable form CA074Me [29] (Figures 1 and 2, *panels D–F*). In addition, we tested the broad-spectrum cysteine protease inhibitor E-64 [34] (Figures 1 and 2, *panels G–I*), the broad-spectrum MMP inhibitor GM6001 [35] (Figures 1 and 2, *panels J–L*), and an inhibitor of the plasminogen cascade aprotinin [36] (Figures 1 and 2, *panels M–O*). At the concentrations used and over the entire time course of the assay, neither the inhibitors nor the diluent (DMSO, 0.1% final concentration) affected the viability of the cells as demonstrated by an absence of staining with propidium iodide (not shown). All of the protease inhibitors significantly reduced the degradation of DQ-collagen IV by the three prostate carcinoma cell lines as can be seen in Figure 1 and is quantified in Table 1. These studies suggest that more than one protease may be responsible for the degradation of collagen IV by the living prostate carcinoma cells, including the cysteine protease cathepsin B. In contrast, degradation of DQ-collagen I by the prostate carcinoma cell lines was not significantly inhibited by all of the protease inhibitors that are effective in reducing the degradation of DQ-collagen IV (Table 1). For DU145 cells, only the broad-spectrum MMP inhibitor GM6001 significantly reduced the degradation of DQ-collagen I (Table 1 and Figure 2*J*), whereas for PC3 cells, only the cathepsin B inhibitors CA074 and CA074Me significantly reduced the degradation (Table 1 and Figure 2*E*). In contrast, degradation of DQ-collagen I by LNCaP cells was significantly reduced (Table 1) by several inhibitors:

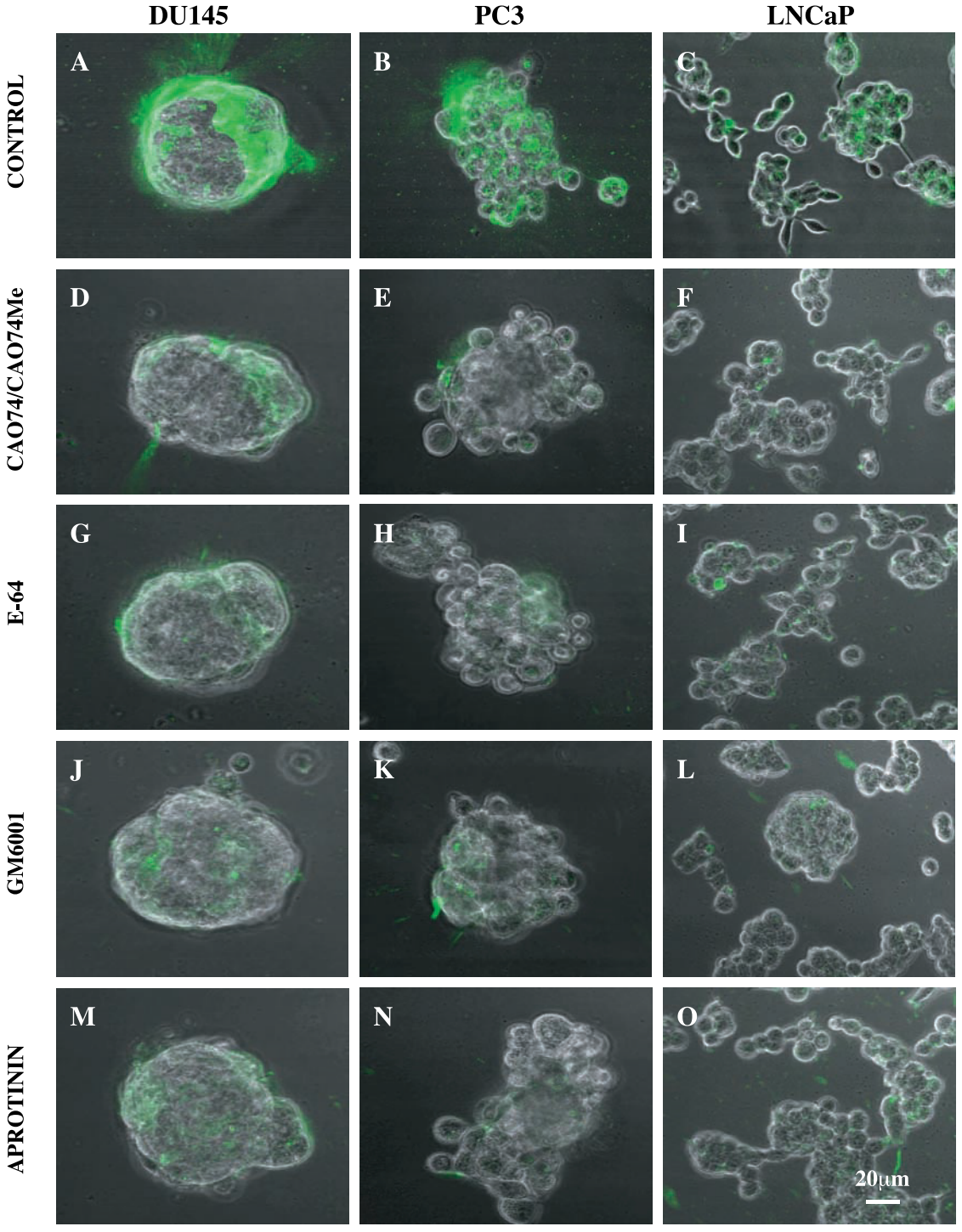

Figure 1. *Protease inhibitors reduce the degradation of DQ-collagen IV by living human DU145, PC3, and LNCaP prostate carcinoma cells. Fluorescence images of DQ-collagen IV degradation products (green) taken at an extended depth of focus are superimposed on phase images of the living tumor cells. Single cell suspensions of prostate carcinoma cells were mixed with diluent (DMSO, 0.1%) or protease inhibitors, plated on DQ-collagen IV/Matrigel–coated coverslips and imaged at 48 hours. Panels A, D, G, J, and M illustrate proteolysis by DU145 cells. Panels B, E, H, K, and N illustrate proteolysis by PC3 cells. Panels C, F, I, L, and O illustrate proteolysis by LNCaP cells. These images are representative of three experiments. Bar = 20 μm.*

broad-spectrum inhibitors of cysteine proteases (Figure 2*I*) and MMPs (Figure 2*L*), and the plasminogen cascade inhibitor aprotinin (Figure 2*O*). These results suggest that degradation of collagen I, the organic matrix of the bone, involves more than one class of proteases, and that the class that is primarily responsible is dependent on the cell line.

Expression of Cathepsin B in Prostate Carcinoma Cells Is Affected by Growth on Collagen I Gels

We have previously reported that interactions of human breast fibroblasts with collagen I can increase the expression of cathepsin B protein, but not cathepsin B transcripts [12]. In the present study, we determined whether interaction with

collagen I affected the levels of cathepsin B expression (transcripts and protein) in prostate carcinoma cells. We isolated total RNA from the prostate cells grown on plastic or collagen I, and evaluated the levels of cathepsin B message by Northern blotting. Two cathepsin B transcripts of 4000 and 2200 nt were detected in DU145 cells (Figure 3, *A* and *C*), but only the smaller predominant transcript was detected in PC3 and LNCaP cells (Figure 3*C*). This is probably due to the lower levels of cathepsin B message in these cells. The levels of cathepsin B transcripts were

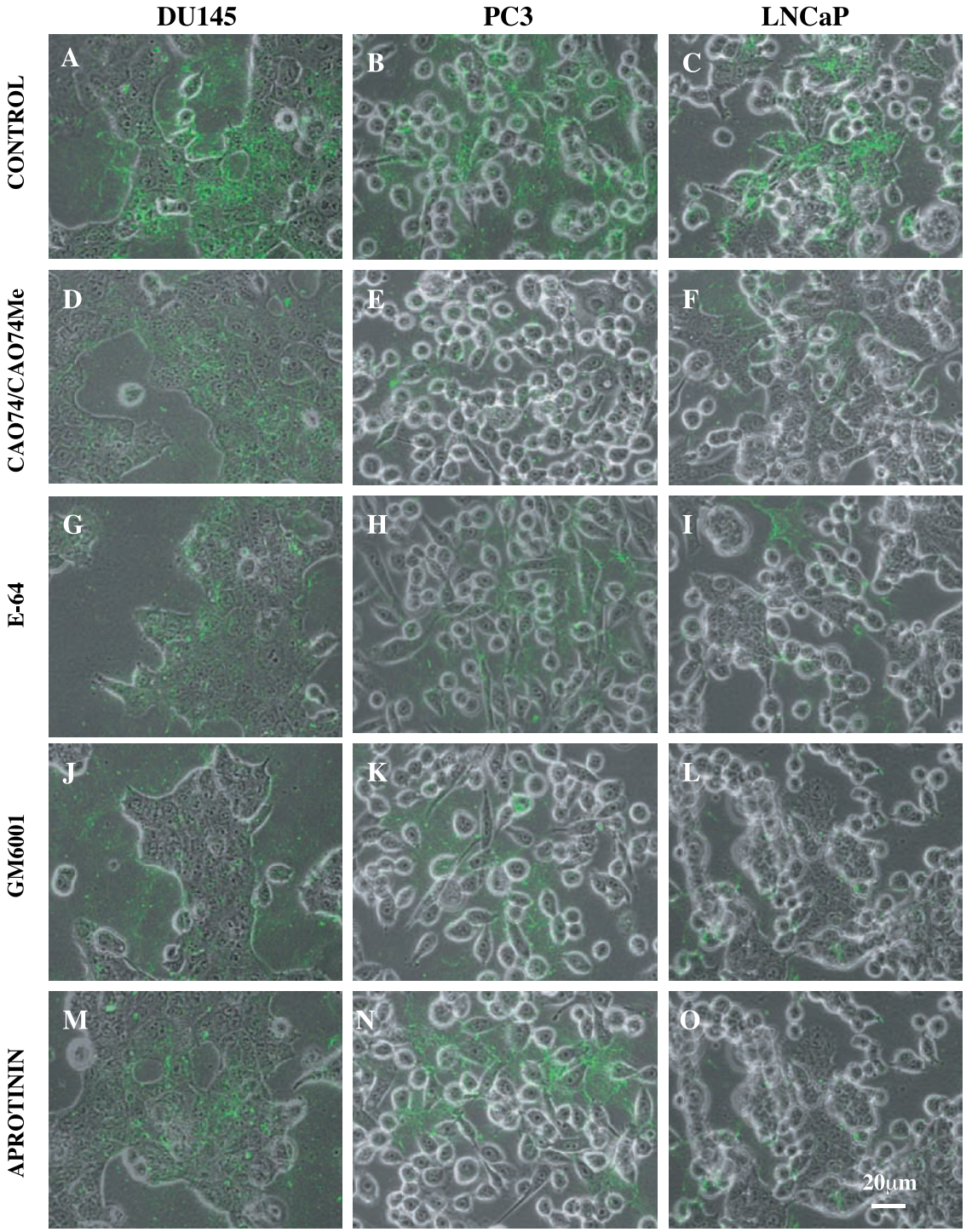

Figure 2. *Degradation of DQ-collagen I by living human DU145, PC3, and LNCaP prostate carcinoma cells is reduced by protease inhibitors. Fluorescence images of DQ-collagen I degradation products (green) taken at an extended depth of focus are superimposed on phase images of the living tumor cells. Single cell suspensions of prostate carcinoma cells were mixed with diluent (DMSO, 0.1%) or protease inhibitors, plated on DQ-collagen I/Matrigel–coated coverslips and imaged at 48 hours. Panels A, D, G, J, and M illustrate proteolysis by DU145 cells. Panels B, E, H, K, and N illustrate proteolysis by PC3 cells. Panels C, F, I, L, and O illustrate proteolysis by LNCaP cells. These images are representative of three experiments. Bar = 20 μm.*

increased in DU145 cells that were cultured on collagen I gels. The ratio of expression of cathepsin B transcripts to that of the transcript for *GAPDH*, a housekeeping gene (Figure 3*B*), indicates that levels of cathepsin B message were increased >2-fold in DU145 cells grown on collagen I gels.

To determine whether the increase in cathepsin B message in DU145 cells led to increased expression of cathepsin B protein, we evaluated the levels of the enzyme by immunoblotting. The mature 31-kDa single-chain and the 26+5/25+5−kDa mature double-chain forms of cathepsin B were present in lysates from DU145 cells, whereas the inactive 43-kDa proform was detectable only in trace amounts (Figure 4*A*, *top panel*), suggesting near-complete processing of the enzyme. We have shown that cathepsin B in normal breast epithelial cells is processed to mature forms within 30 minutes (Sameni and Sloane, unpublished data) (for a recent review on trafficking and processing of cathepsin B, see Ref. [37]). On 12% gels, mature cathepsin B migrates as a 31-kDa single-chain enzyme, and 26- and 25-kDa heavy chains of double-chain cathepsin B; the 5-kDa light chain is not retained on the gels [21]. Cathepsin B protein expression increased more than six-fold in DU145 cells grown on collagen I gels compared to cells grown on tissue culture plastic (Figure 4*A*, *middle panel*). Only procathepsin B was present in overnight conditioned media from DU145 cells grown either on plastic or collagen I gels (Figure 4*B*, *top panel*). Secretion of the inactive proenzyme was increased approximately five-fold when the cells were cultured on the collagen I gels (Figure 4*B*, *middle panel*). These results are similar to the increases observed in the secretion of procathepsin B from human breast fibroblasts grown on collagen I gels [12]. One possible explanation for increased secretion into conditioned media could be stabilization of the proenzyme on interaction with collagen I. Interestingly, overall levels of intracellular and secreted cathepsin B protein in DU145 cells cultured on collagen I gels increased approximately 11-fold, whereas the increase in mRNA levels was only two-fold. This suggests an increase in the translation of cathepsin B in these cells on interaction with collagen I. We have previously reported increases in cathepsin B protein without increases in cathepsin B transcripts in human breast epithelial cells (i.e., MCF 10A) and human breast fibroblasts, thus suggesting posttranscriptional regulation of this enzyme [12,38].

The changes in overall protein expression interaction of DU145 prostate carcinoma cells with collagen I suggest possible changes in cathepsin B activity. To assess enzyme activity, we used a fluorometric assay utilizing a highly selective substrate for cathepsin B, Z-Arg-Arg-NHMec [32,33]. Consistent with the results of immunoblotting, intracellular levels of cathepsin B activity were significantly increased (~2.7-fold) when DU145 cells were cultured on collagen I gels (Figure 4*A*, *bottom panel*). In overnight conditioned media, only the inactive precursor of the enzyme (i.e., procathepsin B) was detected (Figure 4*B*, *bottom panel*). Therefore, we determined the levels of "pepsin-activatable procathepsin B activity" in the conditioned media [12]. We found that there was a five-fold increase in pepsin-activatable procathepsin B activity in the conditioned media of DU145 cells grown on collagen I gels (Figure 4*B*, *bottom panel*; i.e., comparable to the five-fold increase in secretion of procathepsin B protein). Growth of PC3 and LNCaP cells on collagen I gels did not significantly affect the levels of cathepsin B expression and activity (data not shown).

Localization of Cathepsin B in Prostate Carcinoma Cells

Increases in cathepsin B secretion are often associated with altered subcellular localization of the enzyme, namely translocation from the perinuclear region to the cell periphery. Redistribution and secretion of this lysosomal enzyme

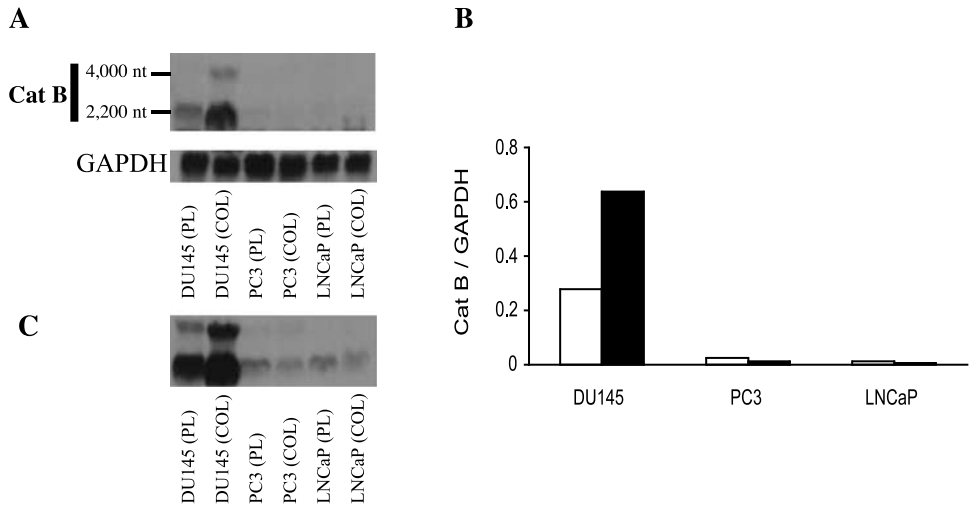

Figure 3. *Cathepsin B mRNA expression increases in DU145 cells grown on collagen I gels. (A). Northern blot demonstrating cathepsin B message in prostate carcinoma cells. Two cathepsin B transcripts of 4000 and 2200 nt were detected in DU145 cells. Twenty micrograms of total RNA was loaded per lane and equal loading was confirmed by probing for GAPDH, a housekeeping gene. To quantify increases in cathepsin B message when DU145 cells are grown in collagen I gels, the ratio of expression of the two cathepsin B transcripts to that of the GAPDH, control was quantified (B) (white, plastic; black, collagen I). (C). Overexposure of blot in panel A to visualize the low levels of cathepsin B message in PC3 and LNCaP cells.*

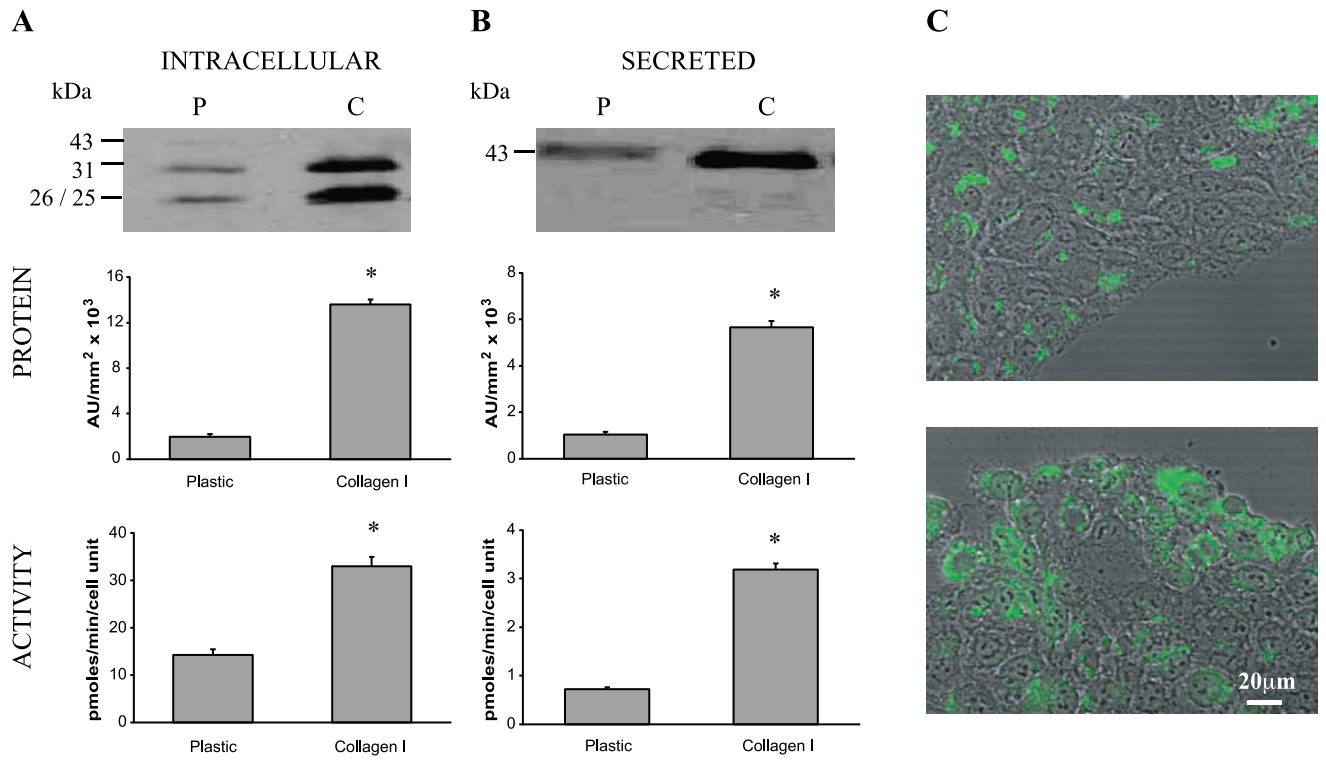

Figure 4. *Levels of cathepsin B protein and activity increase in DU145 cells grown on collagen I gels. (A). Cathepsin B protein (top and middle panels) and activity (bottom panel) in cell lysates from DU145 cells grown on tissue culture plastic (P) or collagen I gels (C). Immunoblot samples were loaded based on DNA concentration (20 μg/lane). The mature 31-kDa single-chain 26+5/25+5−kDa mature double-chain forms, and trace amounts of the inactive 43-kDa proform were detected. Densitometric analyses of cathepsin B bands (43, 31, and 25/26 kDa isoforms) were performed to assess changes in cathepsin B protein expression on interaction with collagen I. Data (expressed as AU/mm^2 × 10^3) are representative of at least three experiments. Activity was measured by fluorometric assay against the cathepsin B substrate Z-Arg-Arg-NHMec. "Cell unit" represents the ratio of milligrams of protein to micrograms of DNA (an index of cell size; see Experimental section). Data are presented as mean ±SD (n = 3) and were repeated at least three times with comparable results. *P ≤ .05 is considered statistically significant. (B). Cathepsin B protein (top and middle panels) and activity (bottom panel) in conditioned media of DU145 cells grown on tissue culture plastic (P) or collagen I gels (C). Only latent procathepsin B was detected in the media; therefore, cathepsin B activity in the conditioned media represents pepsin-activatable cathepsin B. "Cell unit" represents the ratio of milligrams of protein to micrograms of DNA (an index of cell size; see Experimental section). Data are presented as mean ±SD (n = 3) and were repeated at least three times with comparable results. *P ≤ .05 is considered statistically significant. (C). Immunofluorescent staining for intracellular cathepsin B (green) in permeabilized DU145 cells was superimposed on phase contrast images of the cells. Cells were cultured on uncoated (top panel) or collagen I−coated (lower panel) glass coverslips for 48 hours. The cells were observed with a Zeiss LSM 310 microscope in confocal mode at a magnification of ×63 under oil immersion. These images are optical slices that are representative of at least three experiments. Bar = 20 μM.*

have been observed in human colon, breast, prostate, glioma, and esophageal carcinomas, and are reported to parallel malignant progression [14,39−41]. Therefore, in the present study, we analyzed the subcellular localization of cathepsin B in prostate carcinoma cells cultured on glass coverslips either uncoated or coated with a thin layer of collagen I. Growing the cells on glass coverslips does not affect the levels and distribution of cathepsin B compared to cells grown on plastic. DU145, PC3, and LNCaP cells were permeabilized with saponin and stained as described in Experimental section. The antibodies used in immunofluorescent staining detect all forms of the enzyme: inactive proenzyme and the active single-chain and double-chain forms. Staining for cathepsin B in the DU145 cells grown on glass coverslips was vesicular and localized primarily to the perinuclear region of the cells (Figure 4*C*, *top panel*). In DU145 cells cultured on collagen I gels, there was an increased expression of cathepsin B but no apparent changes in cellular localization (Figure 4*C*, *bottom panel*). Images represent a confocal slice through the cells and matrix; hence, the staining pattern is not uniform for all cells. Furthermore, no significant increase in staining intensity for cathepsin B was observed in PC3 and LNCaP cells cultured on collagen I gels (data not shown).

Expression and Activity of Cathepsin B in Prostate Carcinoma Cells Grown on Human Bone

Cathepsin B has been previously shown to degrade collagen I, the organic matrix of the bone, and has been implicated in bone resorption [42−46]. We demonstrated that DU145, PC3, and LNCaP prostate carcinoma cells are capable of degrading collagen I (Figure 2). To investigate an effect of bone microenvironment on tumor cell−associated cathepsin B, we cocultured these prostate carcinoma cell lines with human bone *in vitro* (Figure 5). Immunoblot analysis of conditioned media from the control bone cultures revealed the presence of inactive proenzyme (Figure 5*A*). Additional bands indicated the presence of mature active forms of cathepsin B. These forms are most likely in complex with endogenous inhibitors (e.g., cystatin C) of cathepsin B that are also secreted [47,48] and thus not active, as we were unable to measure cathepsin B activity in conditioned media

in the absence of a pepsin activation step (see results of activity assays below). Culture of DU145 cells in the presence of human bone fragments led to a large increase in the secretion of inactive procathepsin B into conditioned media (Figure 5*A*, *top panel*), as was also observed when DU145 cells were grown in collagen I gels (Figure 4*B*). There was no change in secretion of proenzymes into conditioned media when PC3 or LNCaP cells were cultured on human bone explants (Figure 5*A*). Activity assays on conditioned media were performed in the absence or presence of pepsin in order to activate the latent proenzyme, and only the pepsin-containing samples were found to exhibit cathepsin B activity. Media conditioned by DU145 cells cultured on human bone fragments contained the highest levels of pepsin-activatable cathepsin B activity (i.e., DU145 PC3 = LNCaP) and this activity exceeded the sum of activities in the media of either bone or prostate carcinoma cells cultured alone (Figure 5*B*).

To avoid the issue of complex formation between active enzyme and endogenous inhibitors in conditioned media, we have developed a continuous assay that measures cathepsin B activity produced pericellularly by living cells [32,33]. In this "real-time assay," the rate of secretion of active forms of cathepsin B is measured rather than the accumulation of proenzyme in conditioned media. In the present study, the assay was performed at the end of the 48-hour growth period (i.e., at a time comparable to the analysis of conditioned media). Secretion of active cathepsin B into the pericellular assay buffer was then measured over a further time period of 30 minutes (Figure 5*C*). The results of the "real-time assay" were comparable to those obtained by assaying conditioned media in that there was a significant induction of secretion of active cathepsin B when DU145 cells, but not PC3 or LNCaP cells, were cultured on human bone fragments (Figure 5*C*). Secretion of active cathepsin B could not be measured when any of the three prostate cell lines were cultured on collagen I gels (data not shown). These data suggest that a complete bone microenvironment is necessary to induce the secretion of active cathepsin B.

Expression and Activity of Cathepsin B in Experimental SCID-Human Bone Tumors

Previous studies have shown that injections of human prostate carcinoma cells into the marrow side of human bone fragments implanted in SCID mice result in the formation of

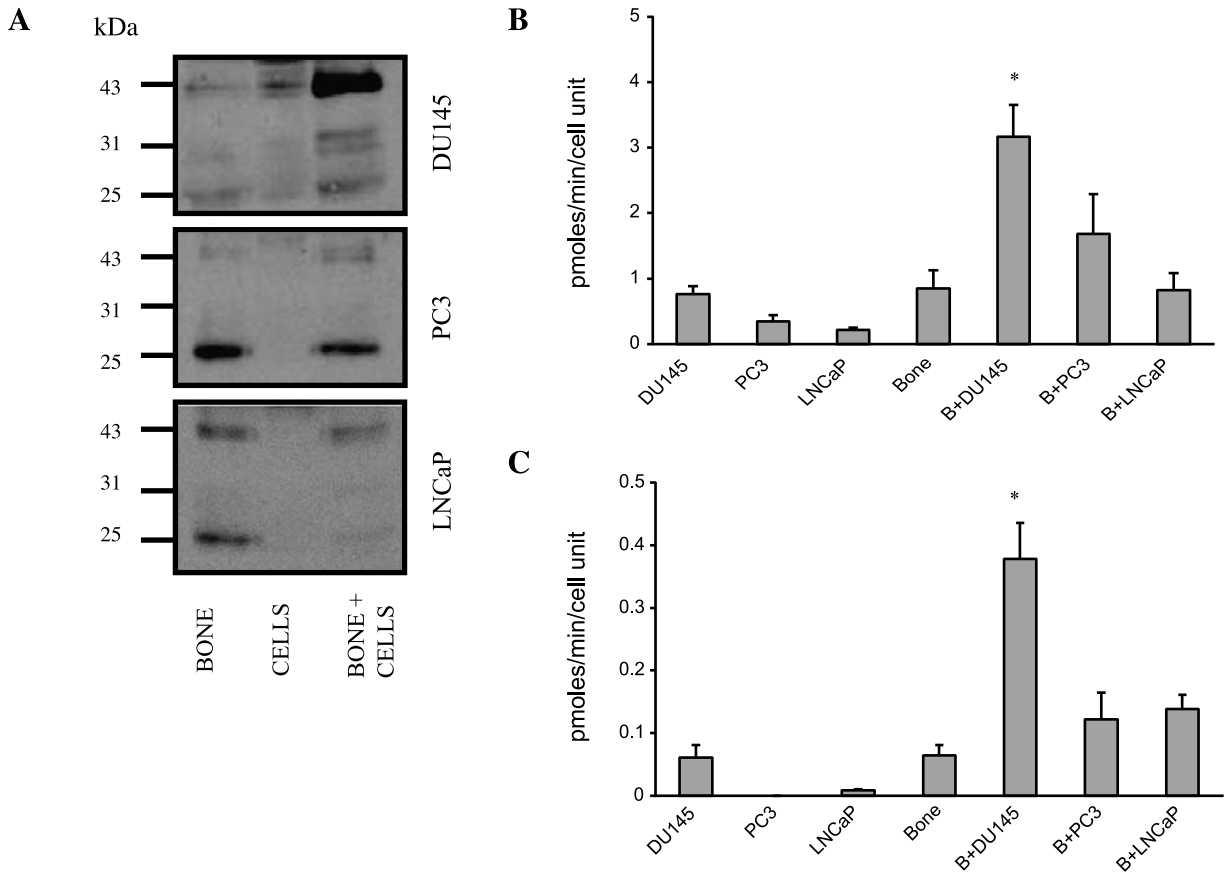

Figure 5. *DU145 cells grown on human bone exhibit increased secretion of cathepsin B. Human prostate carcinoma cells were cultured on bone explants for 48 hours (see Experimental section). (A). Representative immunoblots of conditioned media from three experiments. Samples were loaded based on protein/DNA ratio. (B). Pepsin-activatable cathepsin B activity in 48-hour conditioned media from bones alone, tumor cells alone, and bone (B^+) tumor cell cocultures. (C). Rate of secretion of active cathepsin B from bones alone, tumor cells alone, and bone (B^+) tumor cell cocultures. "Cell unit" represents the ratio of milligrams of protein to micrograms of DNA (an index of cell size; see Experimental). Data are presented as mean ±SD (n = 3) and were repeated at least three times with comparable results. *$P \leq .05$ is considered statistically significant.*

human bone tumors [20]. We have utilized this model in the present study to analyze the effects of an *in vivo* human bone microenvironment on cathepsin B expression and activity in human prostate tumors. In agreement with the results of our *in vitro* studies, active forms (31-kDa single chain and 26/25-kDa double chain) of cathepsin B were found by immunoblotting in extracts of control human bone fragments (Figure 6, *A* and *B*). A dramatic (>10-fold) increase in cathepsin B protein was observed in DU145 bone tumors compared to the control bone samples (Figure 6*C*). Significant increases in the expression of the enzyme were also found in PC3 and LNCaP bone tumors—effects that were not visible on the interaction of PC3 and LNCaP cells with collagen I or human bone *in vitro*. Levels of cathepsin B expression in human bone tumors corresponded to levels of cathepsin B activity (DU145 > PC3 = LNCaP; Figure 6*D*). The significant increase in cathepsin B in all of the prostate bone tumors indicates that interactions of the stroma and host tissues with the tumor may regulate the expression of this enzyme in prostate cancer bone metastases.

Localization of Cathepsin B mRNA and Protein in Human Bone Tumors

The three prostate carcinoma cell lines formed large, well-encapsulated, solid tumors on the implanted bone. On histologic examination, all bone tumors exhibited variable degrees of osteolytic activity (Figure 7, *B–D*). DU145 and PC3 tumors, as previously reported [20], appeared to be osteolytic in nature; however, in DU145 tumors, visible bone fragments were still apparent at 6 weeks after tumor cell injection (Figure 7*B*). At 6 weeks after injection of PC3 cells, bone fragments were not observed in most tumors (Figure 7*C*). LNCaP tumors, which have previously been reported to be of an osteoblastic/osteolytic type, appeared to degrade bone, as determined by H&E staining, but no evidence of new bone formation was found (Figure 7*D*). *In situ* hybridization and immunohistochemical staining revealed undetectable levels of cathepsin B message and relatively low levels of cathepsin B protein in bone fragments from control mice (Figure 7, *E* and *I*). Cathepsin B protein appeared to be localized to the lacunae areas of the bone (Figure 7*I*). When compared to bone fragments from control mice, cathepsin B mRNA and protein levels were significantly increased in all bone tumors. Cathepsin B message and protein appeared to be mainly localized to the tumor cells, and not to the surrounding stromal cells (Figure 7, *F–H* and *J–L*). The residual bone fragments that were visible in some tumors showed minimal staining for cathepsin B in the lacunae, consistent with the staining in bone fragments from control mice. We did not observe a comparable increase in expression of either cathepsin B message or protein in subcutaneous tumors of the three cell lines (Figure 8), again consistent with the importance of bone microenvironment in regulating cathepsin B expression in prostate cancer. Overall, immunostaining for cathepsin B correlated with our immunoblotting and activity assays. The exception was LNCaP bone tumors (Figure 7, *H* and *L*), in which there was intense staining for cathepsin B. One possible explanation for this intense staining could be background fluorescence due to increased angiogenesis in LNCaP tumors. Neovessels in some tumors (e.g., gliomas) [49] have previously been shown to exhibit intense staining for cathepsin B. On histologic examination, these tumors appear to have an increased number of red blood cells and angiogenic vasculature—an effect that is not observable in DU145 and PC3 tumors.

Discussion

The bone marrow microenvironment has been hypothesized to favor the growth of prostate cancer cells that enter the bone marrow from the circulation [50,51]. Skeletal metastasis is a complex, multistep process, the mechanisms of which are not fully understood. Clinically, prostate cancer bone metastases are predominantly osteoblastic in nature; however, osteolytic bone resorption is still an important factor in bone colonization by prostate cancer cells and numerous studies demonstrate the presence of osteolytic activity in human clinical specimens [52–56]. Without bone resorption, growth factors are less available to metastatic cancer cells, leading to a widely accepted dogma that prostate cancer is dependent on osteoclasts for expansion in the bone marrow and subsequent progression of osteolytic metastases [6]. Osteoclasts attach themselves to the bone surface and create an acidic environment that allows for matrix demineralization. They also secrete proteolytic enzymes, including MMPs and cysteine proteases, that aid in matrix degradation [57–62]. The most abundant cysteine protease found in osteoclasts is cathepsin K, a protease implicated in bone resorption [63–65]. Cathepsin B has also been found in the extracellular resorption lacunae of osteoclasts, and has been implicated in osteoclastic bone resorption [42,45,46]. Interestingly, osteoclast resorption activity has been shown to be reduced by inhibition of cathepsin B or TRAP in isolated osteoclasts [66–68]. Recently, cathepsin B in rheumatoid arthritis synovial fluid has been demonstrated to participate in the degradation of subchondral bone collagen [66].

In the present study, we examined the proteolytic potential of prostate carcinoma cells and demonstrated that these cells are not only able to degrade basement membrane collagen IV, but also collagen I, a major component of bone matrix and connective tissues. Using a novel confocal assay developed in our laboratory that allows one to image matrix degradation by living cells [25,26], we showed that degradation of collagen I by the prostate carcinoma cells depends on various classes of proteases. Our results suggested that during tumor-mediated proteolysis of collagen I, there may be an interplay between cathepsin B and other proteases, including MMPs—enzymes known to be activated by cathepsin B [18,19]. These results also indicate that tumor cell–mediated proteolysis might be an important factor in the ability of prostate cancer cells to colonize the bone and participate in osteoclast-mediated osteolysis. Some studies have suggested such roles for tumor cell–expressed degradative enzymes, including matrix metalloproteases, serine proteases (i.e., uPA), and cysteine proteases (i.e., cathepsin K)

in the establishment of prostate carcinoma cells within the bone marrow [67,68].

Interaction with extracellular matrix can also regulate the expression of proteases in a variety of cells including fibroblasts and tumor cells [9,10,69–71]. Our studies have shown previously that the growth of human breast fibroblasts in collagen I gels alters the expression of cathepsin B [12]. In the present study, altered cathepsin B expression and activity were demonstrated on the interaction of DU145 cells with collagen I and the human bone, but not of PC3 or LNCaP cells

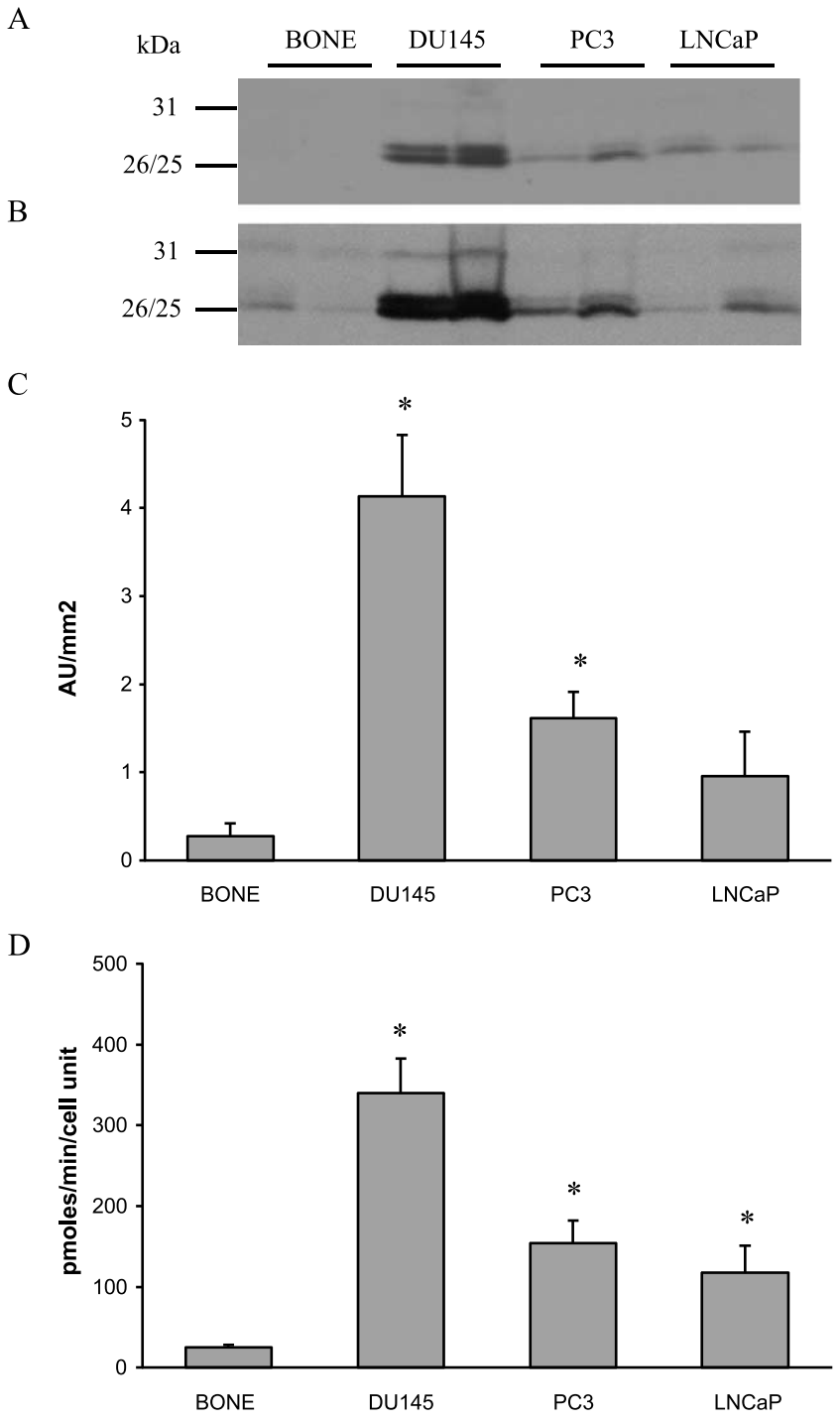

Figure 6. *Cathepsin B expression and activity are increased in human prostate carcinoma bone tumors. (A). Cathepsin B expression in extracts from human bone tumors was assessed by immunoblotting. Two tumors from each group were analyzed, and samples were loaded based on protein/DNA ratio. For purposes of clarity, we purposefully loaded half as much protein from the DU145 bone tumor samples as we did for the other bone tumor samples. (B). An overexposed blot used to demonstrate the presence of active forms of cathepsin B in control bone samples. (C). Densitometric analysis of cathepsin B isoforms was performed to assess changes in cathepsin B protein expression in bone tumors as compared to bone fragments in control mice. Data (expressed as AU/mm^2) are representative of at least three experiments. (D) Cathepsin B activity in bone tumors was measured by fluorometric assay against the cathepsin B substrate Z-Arg-Arg-NHMec. "Cell unit" represents the ratio of milligram of protein to micrograms of DNA (an index of cell size; see Experimental section). Data are presented as mean ±SD (n = 3) and were repeated at least three times with comparable results. *P ≤ .05 is considered statistically significant.*

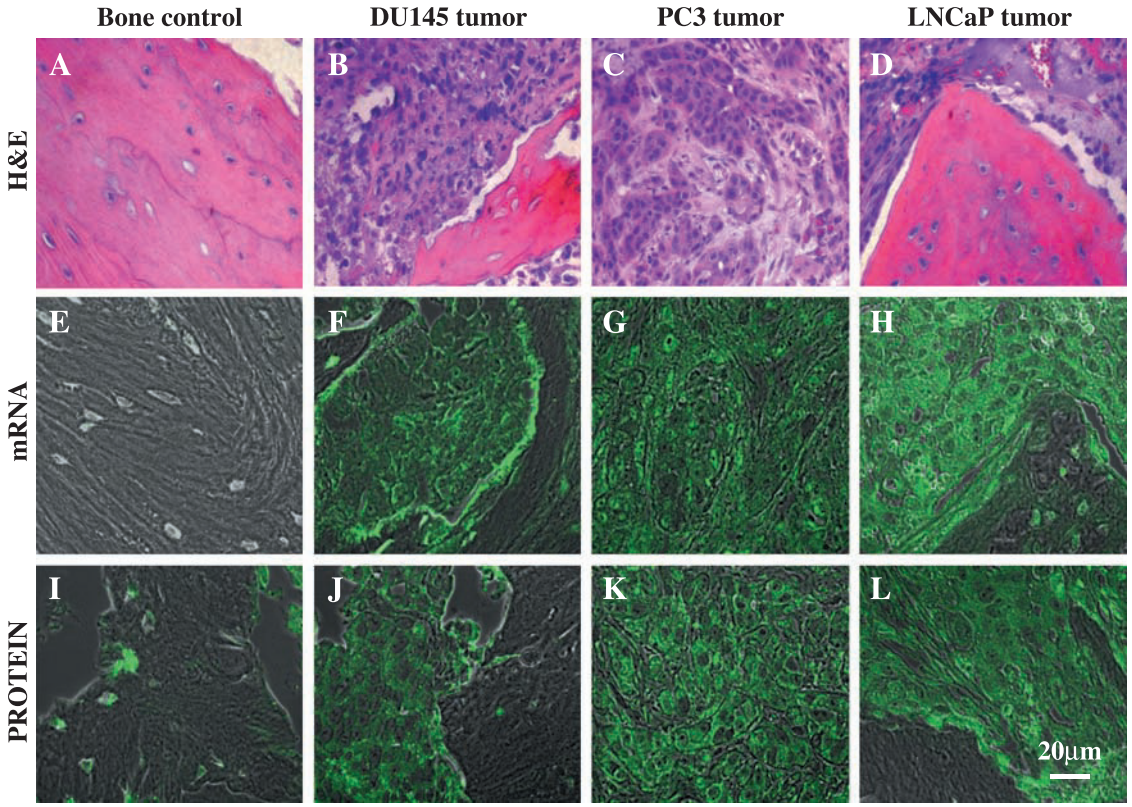

Figure 7. *Levels of cathepsin B expression in human prostate carcinoma bone tumor xenografts are high. Paraffin-fixed, decalcified, and dehydrated serial sections of each tumor were analyzed by H&E staining, in situ hybridization, and immunohistochemistry. (A–D) H&E staining, ×40. (E–H) Immunofluorescent staining for cathepsin B mRNA expression. (I–L) Cathepsin B protein expression. Bar = 20 μM. Panels A, E, and I illustrate human bone fragments from control mice. Panels B, F, and J illustrate DU145 bone tumors with evidence of osteolysis. Panels C, G, and K illustrate PC3 bone tumors, with tumor cells and fibrous stroma, but no remaining bone fragments. Panels D, H, and L illustrate LNCaP bone tumors with evidence of osteolysis, but no apparent new bone formation. The slides were observed with a Zeiss LSM 310 microscope in confocal mode at a magnification of ×63 under oil immersion. These images are optical slices that are representative of at least three experiments.*

with either collagen I or the human bone *in vitro*. Interestingly, the DU145 cell line has also been shown to express uPA/uPAR, a protease system that can be activated by cathepsin B [15] and one implicated in the proliferation and metastasis of cancer cells. Elevated levels of uPA have been detected in breast, lung, colon, and prostate bone metastases [72–74]. Recently, overexpression of maspin, a serine protease inhibitor [75], in tumor cells was shown to inhibit motility, invasion, angiogenesis, and bone degradation [76–78]. Cathepsin B–mediated activation of pro-uPA leads to activation of TGF-β [17], a growth factor implicated in interactions between prostate cancer cell lines and bone marrow stromal cells [79]. DU145 cells have been shown to express the highest levels of TGF-β among the three prostate cell lines analyzed in the present study [80]. TGF-β has also been implicated in the regulation of the SMAD family of transcription factors [81], an activity further increased by Ets-1 [82]. Interestingly, Ets-1 is a transcription factor that regulates cathepsin B expression [83]. In addition, both TGF-β and Ets-1 have been implicated in the regulation of expression of uPA [84,85]. A growing body of evidence suggests that a functional interaction between TGF-β and Ets-1 is important for the acquisition of an invasive phenotype by tumor cells.

For instance, expansion of breast cancer cells in the bone has been shown to depend on parathyroid hormone-related protein (PTHrP), the expression of which is stimulated by TGF-β through SMAD/Ets-1 synergism [82,86]. This suggests the importance of Ets-1 in the homing of cancer cells in the bone microenvironment. Cell adhesion to bone matrix protein, collagen type I, has been shown to induce Ets-1 expression in endothelial cells, a process ultimately leading to the activation of MMP-1 [87]. Given the widely demonstrated involvement of Ets-1 in the transcriptional regulation of matrix-degrading enzymes, it is possible that regulation by Ets-1 could be responsible for the unique changes in cathepsin B expression and activity that occur on interaction of DU145 cells with bone matrix.

Differences in tumor cell–associated cathepsin B among the three cell lines may be regulated by integrins, which are important mediators of tumor cell/bone or tumor cell/collagen I associations [8]. We have already shown that the interaction of collagen I with integrins alters cathepsin B expression and secretion in human breast fibroblasts [12]. Modulation of other proteases, including MMPs [88,89] and the uPA/uPAR system by integrins [90,91], has also been demonstrated. In prostate cancer, integrins have been shown to mediate the preferential adhesion of cancer cells to bone marrow endothelium [50,51]. A major contributor to this binding is $\alpha_2\beta_1$, an integrin expressed by DU145 and PC3 cells, but not by LNCaP cells, and also one implicated in the regulation of

procathepsin B secretion by human breast fibroblasts [12]. Interestingly, *de novo* synthesis of $\alpha_2\beta_1$ subunits is stimulated by TGF-β [92], a growth factor found in higher amounts in DU145 than PC3 cells [80]. Signaling through $\alpha_v\beta_3$, an integrin commonly expressed by DU145 and PC3 cells [93,94], is yet another mechanism implicated in prostate cancer metastasis to the bones [95]. Blocking $\alpha_v\beta_3$ integrin in DU145 cells almost completely abolishes the adhesion of these cells to crude bone protein extract [96]. Moreover, inhibition of $\alpha_v\beta_3$ integrin in the bone environment results in reduced recruitment of osteoclasts, reduced osteolysis, and growth of tumor cells in the bone [97].

An interesting effect observed when DU145 cells interacted with the human bone but not with the pure bone matrix, collagen I, was secretion of active cathepsin B. Mechanisms for secretion of active cathepsin B are not well understood; however, procathepsin B is secreted constitutively and secretion of active cathepsin B can be induced (e.g., by lowering the pericellular pH) [98]. It is possible that the enzyme is processed through a classic lysosomal pathway and secreted by a retrograde mechanism. Lysosomal exocytosis and secretion of mature active enzyme due to fusion of lysosomes with secretory granules have been observed in rat exocrine pancreas [99]. The presence of active cathepsin B pericellularly might also reflect the activation of procathepsin B on the cell surface (for a recent review on trafficking and processing of cathepsin B, see Ref. [37]). Secretion of active enzyme from cells interacting with human bone, but not from cells interacting with pure collagen I, suggests that it is not the bone matrix itself, but the metabolically rich bone microenvironment that is responsible. Our working hypothesis that tumor–stromal and tumor–host interactions modulate the expression of cathepsin B in prostate tumors was further supported by our *in vivo* studies using the SCID-human model of prostate cancer bone metastasis [20]. Here we demonstrated an upregulation of cathepsin B levels in bone tissues colonized by human prostate carcinoma cells. Increased cathepsin B expression and activity were

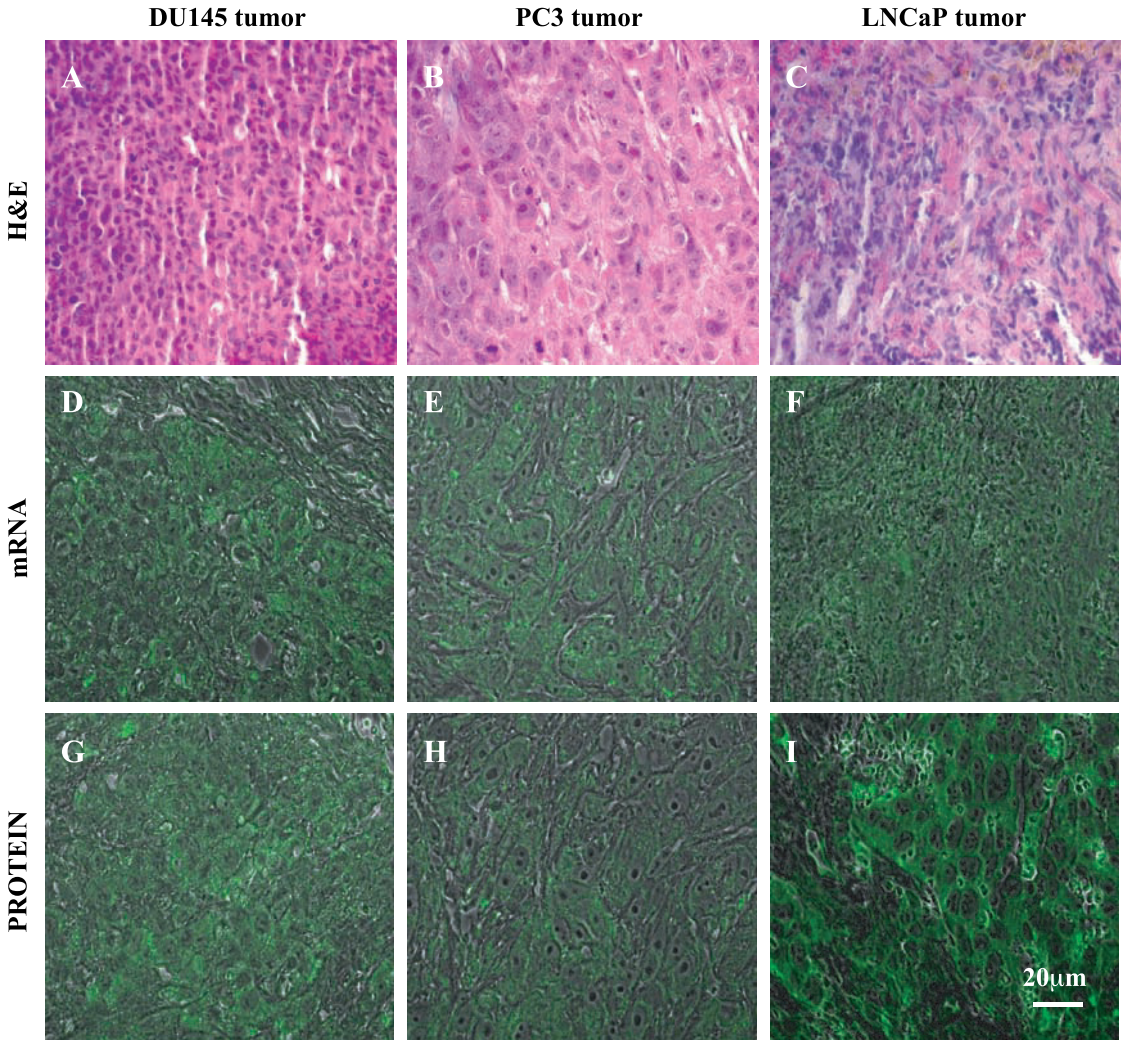

Figure 8. *Levels of cathepsin B expression in subcutaneous human prostate tumor xenografts. (A–C) H&E staining, ×40. Immunofluorescent staining for cathepsin B mRNA (D–F) and cathepsin B protein (G–I). Bar = 20 μM. Panels A, D, and G illustrate DU145 subcutaneous tumors. Panels B, E, and H illustrate PC3 subcutaneous tumors. Panels C, F, and I illustrate LNCaP subcutaneous tumors. The slides were observed with a Zeiss LSM 310 microscope in confocal mode at a magnification of ×63 under oil immersion. These images are optical slices that are representative of at least three experiments.*

observed in all tumor tissues, including PC3 and LNCaP tumors, which show relatively low levels of the enzyme *in vitro*. It is somewhat surprising and yet unclear why PC3 cells that were isolated from a bone metastasis exhibit upregulation of cathepsin B *in vivo*, yet do not respond to bone matrix components *in vitro*. It is possible that cathepsin B in these cells is regulated by nonmatrix components of the bone microenvironment. One such candidate is osteoprotegerin, a protein shown to downregulate expression of the cysteine protease cathepsin K in osteoclast cultures [100]. Our future studies will include the analysis of the effects of osteoprotegerin and other bone proteins on cathepsin B expression in prostate cancer.

To the best of our knowledge, the present study is the first proof that the tumor microenvironment can modulate the expression of a cysteine protease, in this case cathepsin B—a finding that might translate into novel therapeutic agents for treatment of prostate cancer patients.

Acknowledgements

We gratefully acknowledge Kamiar Moin for assistance with the Zeiss LSM-310 confocal microscope.

References

[1] Buck MR, Karustis DG, Day NA, Honn KV, and Sloane BF (1992). Degradation of extracellular-matrix proteins by human cathepsin B from normal and tumour tissues. *Biochem J* **282,** 273–278.

[2] Johnsen M, Lund LR, Romer J, Almholt K, and Dano K (1998). Cancer invasion and tissue remodeling: common themes in proteolytic matrix degradation. *Curr Opin Cell Biol* **10,** 667–671.

[3] Garcia M, Platet N, Liaudet E, Laurent V, Derocq D, Brouillet JP, and Rochefort H (1996). Biological and clinical significance of cathepsin D in breast cancer metastasis. *Stem Cells* **14,** 642–650.

[4] Khan A, Krishna M, Baker SP, Malhothra R, and Banner BF (1998). Cathepsin B expression and its correlation with tumor-associated laminin and tumor progression in gastric cancer. *Arch Pathol Lab Med* **122,** 172–177.

[5] Zeng ZS, Cohen AM, and Guillem JG (1999). Loss of basement membrane type IV collagen is associated with increased expression of metalloproteinases 2 and 9 (MMP-2 and MMP-9) during human colorectal tumorigenesis. *Carcinogenesis* **20,** 749–755.

[6] Yoneda T (1998). Cellular and molecular mechanisms of breast and prostate cancer metastasis to bone. *Eur J Cancer* **34,** 240–245.

[7] Klein CE, Dressel D, Steinmayer T, Mauch C, Eckes B, Krieg T, Bankert RB, and Weber L (1991). Integrin alpha 2 beta 1 is upregulated in fibroblasts and highly aggressive melanoma cells in three-dimensional collagen lattices and mediates the reorganization of collagen I fibrils. *J Cell Biol* **115,** 1427–1436.

[8] Kostenuik PJ, Sanchez-Sweatman O, Orr FW, and Singh G (1996). Bone cell matrix promotes the adhesion of human prostatic carcinoma cells *via* the alpha 2 beta 1 integrin. *Clin Exp Metastasis* **14,** 19–26.

[9] Stanton H, Gavrilovic J, Atkinson SJ, d'Ortho MP, Yamada KM, Zardi L, and Murphy G (1998). The activation of ProMMP-2 (gelatinase A) by HT1080 fibrosarcoma cells is promoted by culture on a fibronectin substrate and is concomitant with an increase in processing of MT1-MMP (MMP-14) to a 45 kDa form. *J Cell Sci* **111,** 2789–2798.

[10] Mauch C, Adelmann-Grill B, Hatamochi A, and Krieg T (1989). Collagenase gene expression in fibroblasts is regulated by a three-dimensional contact with collagen. *FEBS Lett* **250,** 301–305.

[11] Khan KM and Falcone DJ (1997). Role of laminin in matrix induction of macrophage urokinase-type plasminogen activator and 92-kDa metalloproteinase expression. *J Biol Chem* **272,** 8270–8275.

[12] Koblinski JE, Dosescu J, Sameni M, Moin K, Clark K, and Sloane BF (2002). Interaction of human breast fibroblasts with collagen I increases secretion of procathepsin B. *J Biol Chem* **277,** 32220–32227.

[13] Sinha AA, Gleason DF, Deleon OF, Wilson MJ, and Sloane BF (1993). Localization of a biotinylated cathepsin B oligonucleotide probe in human prostate including invasive cells and invasive edges by *in situ* hybridization. *Anat Rec* **235,** 233–240.

[14] Sinha AA, Wilson MJ, Gleason DF, Reddy PK, Sameni M, and Sloane BF (1995). Immunohistochemical localization of cathepsin B in neoplastic human prostate. *Prostate* **26,** 171–178.

[15] McGowen R, Biliran H Jr, Sager R, and Sheng S (2000). The surface of prostate carcinoma DU145 cells mediates the inhibition of urokinase-type plasminogen activator by maspin. *Cancer Res* **60,** 4771–4778.

[16] Kobayashi H, Moniwa N, Sugimura M, Shinohara H, Ohi H, and Terao T (1993). Increased cell-surface urokinase in advanced ovarian cancer. *Jpn J Cancer Res* **84,** 633–640.

[17] Guo M, Mathieu PA, Linebaugh B, Sloane BF, and Reiners JJ Jr (2002). Phorbol ester activation of a proteolytic cascade capable of activating latent transforming growth factor-betaL a process initiated by the exocytosis of cathepsin B. *J Biol Chem* **277,** 14829–14837.

[18] Murphy G, Ward R, Gavrilovic J, and Atkinson S (1992). Physiological mechanisms for metalloproteinase activation. *Matrix Suppl* **1,** 224–230.

[19] Kostoulas G, Lang A, Nagase H, and Baici A (1999). Stimulation of angiogenesis through cathepsin B inactivation of the tissue inhibitors of matrix metalloproteinases. *FEBS Lett* **455,** 286–290.

[20] Nemeth JA, Harb JF, Barroso U Jr, He Z, Grignon DJ, and Cher ML (1999). Severe combined immunodeficient-hu model of human prostate cancer metastasis to human bone. *Cancer Res* **59,** 1987–1993.

[21] Moin K, Day NA, Sameni M, Hasnain S, Hirama T, and Sloane BF (1992). Human tumour cathepsin B. Comparison with normal liver cathepsin B. *Biochem J* **285,** 427–434.

[22] Stone KR, Mickey DD, Wunderli H, Mickey GH, and Paulson DF (1978). Isolation of a human prostate carcinoma cell line (DU 145). *Int J Cancer* **21,** 274–281.

[23] Kaighn ME, Narayan KS, Ohnuki Y, Lechner JF, and Jones LW (1979). Establishment and characterization of a human prostatic carcinoma cell line (PC-3). *Invest Urol* **17,** 16–23.

[24] Horoszewicz JS, Leong SS, Chu TM, Wajsman ZL, Friedman M, Papsidero L, Kim U, Chai LS, Kakati S, Arya SK, and Sandberg AA (1980). The LNCaP cell line—a new model for studies on human prostatic carcinoma. *Prog Clin Biol Res* **37,** 115–132.

[25] Sameni M, Moin K, and Sloane BF (2000). Imaging proteolysis by living human breast cancer cells. *Neoplasia* **2,** 496–504.

[26] Sameni M, Dosescu J, and Sloane BF (2001). Imaging proteolysis by living human glioma cells. *Biol Chem* **382,** 785–788.

[27] Sameni M, Dosescu J, Moin K, and Sloane BF (2003). Functional imaging of proteolysis: stromal and inflammatory cells increase tumor proteolysis. *Mol Imaging* **2,** 159–175.

[28] Murata M, Miyashita S, Yokoo C, Tamai M, Hanada K, Hatayama K, Towatari T, Nikawa T, and Katunuma N (1991). Novel epoxysuccinyl peptides. Selective inhibitors of cathepsin B, *in vitro*. *FEBS Lett* **280,** 307–310.

[29] Yamamoto A, Hara T, Tomoo K, Ishida T, Fujii T, Hata Y, Murata M, and Kitamura K (1997). Binding mode of CA074, a specific irreversible inhibitor, to bovine cathepsin B as determined by X-ray crystal analysis of the complex. *J Biochem (Tokyo)* **121,** 974–977.

[30] Montaser M, Lalmanach G, and Mach L (2002). CA-074, but not its methyl ester CA-074Me, is a selective inhibitor of cathepsin B within living cells. *Biol Chem* **383,** 1305–1308.

[31] Downs TR and Wilfinger WW (1983). Fluorometric quantification of DNA in cells and tissue. *Anal Biochem* **131,** 538–547.

[32] Linebaugh BE, Sameni M, Day NA, Sloane BF, and Keppler D (1999). Exocytosis of active cathepsin B enzyme activity at pH 7.0, inhibition and molecular mass. *Eur J Biochem* **264,** 100–109.

[33] Hulkower KI, Butler CC, Linebaugh BE, Klaus JL, Keppler D, Giranda VL, and Sloane BF (2000). Fluorescent microplate assay for cancer cell–associated cathepsin B. *Eur J Biochem* **267,** 4165–4170.

[34] Barrett AJ, Kembhavi AA, Brown MA, Kirschke H, Knight CG, Tamai M, and Hanada K (1982). L-*trans*-epoxysuccinyl-leucylamido(4-guanidino)-butane (E-64) and its analogues as inhibitors of cysteine proteinases including cathepsins B, H and L. *Biochem J* **201,** 189–198.

[35] Galardy RE, Grobelny D, Foellmer HG, and Fernandez LA (1994). Inhibition of angiogenesis by the matrix metalloprotease inhibitor *N*-[2*R*-2-(hydroxamidocarbonymethyl)-4-methylpentanoyl)]-L-tryptophan methylamide. *Cancer Res* **54,** 4715–4718.

[36] Gebhard W, Tschesche H, and Fritz H (1986). Biochemistry of aprotinin and aprotinin-like inhibitors. *Proteinase Inhibitors* pp.375–388 Elsevier Science, New York.

[37] Roshy S, Sloane BF, and Moin K (2003). Pericellular cathepsin B and malignant progression. *Cancer Metastasis Rev* **22,** 271–286.

[38] Sloane BF, Moin K, Sameni M, Tait LR, Rozhin J, and Ziegler G (1994). Membrane association of cathepsin B can be induced by transfection of human breast epithelial cells with c-*Ha-ras* oncogene. *J Cell Sci* **107,** 373–384.

[39] Sameni M, Elliott E, Ziegler G, Fortgens PH, Dennison C, and Sloane BF (1995). Cathepsin B and D are localized at the surface of human breast cancer cells. *Pathol Oncol Res* **1,** 43–53.

[40] Campo E, Munoz J, Miquel R, Palacin A, Cardesa A, Sloane BF, and Emmert-Buck MR (1994). Cathepsin B expression in colorectal carcinomas correlates with tumor progression and shortened patient survival. *Am J Pathol* **145,** 301–309.

[41] Rempel SA, Rosenblum ML, Mikkelsen T, Yan PS, Ellis KD, Golembieski WA, Sameni M, Rozhin J, Ziegler G, and Sloane BF (1994). Cathepsin B expression and localization in glioma progression and invasion. *Cancer Res* **54,** 6027–6031.

[42] Everts V, Delaisse JM, Korper W, and Beertsen W (1998). Cysteine proteinases and matrix metalloproteinases play distinct roles in the subosteoclastic resorption zone. *J Bone Miner Res* **13,** 1420–1430.

[43] Hill PA, Buttle DJ, Jones SJ, Boyde A, Murata M, Reynolds JJ, and Meikle MC (1994). Inhibition of bone resorption by selective inactivators of cysteine proteinases. *J Cell Biochem* **56,** 118–130.

[44] Goto T, Kiyoshima T, Moroi R, Tsukuba T, Nishimura Y, Himeno M, Yamamoto K, and Tanaka T (1994). Localization of cathepsins B, D, and L in the rat osteoclast by immuno-light and -electron microscopy. *Histochemistry* **101,** 33–40.

[45] Schutze N, Oursler MJ, Nolan J, Riggs BL, and Spelsberg TC (1995). Zeolite A inhibits osteoclast-mediated bone resorption *in vitro*. *J Cell Biochem* **58,** 39–46.

[46] Everts V, Korper W, Jansen DC, Steinfort J, Lammerse I, Heera S, Docherty AJ, and Beertsen W (1999). Functional heterogeneity of osteoclasts: matrix metalloproteinases participate in osteoclastic resorption of calvarial bone but not in resorption of long bone. *FASEB J* **13,** 1219–1230.

[47] Heidtmann HH, Salge U, Abrahamson M, Bencina M, Kastelic L, Kopitar-Jerala N, Turk V, and Lah TT (1997). Cathepsin B and cysteine proteinase inhibitors in human lung cancer cell lines. *Clin Exp Metastasis* **15,** 368–381.

[48] Burnett D, Abrahamson M, Devalia JL, Sapsford RJ, Davies RJ, and Buttle DJ (1995). Synthesis and secretion of procathepsin B and cystatin C by human bronchial epithelial cells *in vitro*: modulation of cathepsin B activity by neutrophil elastase. *Arch Biochem Biophys* **317,** 305–310.

[49] Mai J, Sameni M, Mikkelsen T, and Sloane BF (2002). Degradation of extracellular matrix protein tenascin C by cathepsin B: an interaction involved in progression of gliomas. *Biol Chem* **383,** 1407–1413.

[50] Scott LJ, Clarke NW, George NJ, Shanks JH, Testa NG, and Lang SH (2001). Interactions of human prostatic epithelial cells with bone marrow endothelium: binding and invasion. *Br J Cancer* **84,** 1417–1423.

[51] Lehr JE and Pienta KJ (1998). Preferential adhesion of prostate cancer cells to a human bone marrow endothelial cell line. *J Natl Cancer Inst* **90,** 118–123.

[52] Saad F, Gleason DM, Murray R, Tchekmedyian S, Venner P, Lacombe L, Chin JL, Vinholes JJ, Goas JA, and Chen B (2002). A randomized, placebo-controlled trial of zoledronic acid in patients with hormone-refractory metastatic prostate carcinoma. *J Natl Cancer Inst* **94,** 1458–1468.

[53] Garnero P, Buchs N, Zekri J, Rizzoli R, Coleman RE, and Delmas PD (2000). Markers of bone turnover for the management of patients with bone metastases from prostate cancer. *Br J Cancer* **82,** 858–864.

[54] Berruti A, Dogliotti L, Bitossi R, Fasolis G, Gorzegno G, Bellina M, Torta M, Porpiglia F, Fontana D, and Angeli A (2000). Incidence of skeletal complications in patients with bone metastatic prostate cancer and hormone refractory disease: predictive role of bone resorption and formation markers evaluated at baseline. *J Urol* **164,** 1248–1253.

[55] Akimoto S, Furuya Y, Akakura K, and Ito H (1998). Comparison of markers of bone formation and resorption in prostate cancer patients to predict bone metastasis. *Endocr J* **45,** 97–104.

[56] Revilla M, Arribas I, Sanchez-Chapado M, Villa LF, Bethencourt F, and Rico H (1998). Total and regional bone mass and biochemical markers of bone remodeling in metastatic prostate cancer. *Prostate* **35,** 243–247.

[57] Nemeth JA, Yousif R, Herzog M, Che M, Upadhyay J, Shekarriz B, Bhagat S, Mullins C, Fridman R, and Cher ML (2002). Matrix metalloproteinase activity, bone matrix turnover, and tumor cell proliferation in prostate cancer bone metastasis. *J Natl Cancer Inst* **94,** 17–25.

[58] Inui T, Ishibashi O, Origane Y, Fujimori K, Kokubo T, and Nakajima M (1999). Matrix metalloproteinases and lysosomal cysteine proteases in osteoclasts contribute to bone resorption through distinct modes of action. *Biochem Biophys Res Commun* **258,** 173–178.

[59] Delaisse JM, Andersen TL, Engsig MT, Henriksen K, Troen T, and Blavier L (2003). Matrix metalloproteinases (MMP) and cathepsin K contribute differently to osteoclastic activities. *Microsc Res Technol* **61,** 504–513.

[60] Keller ET (2002). The role of osteoclastic activity in prostate cancer skeletal metastases. *Drugs Today (Barcelona)* **38,** 91–102.

[61] Tezuka K, Tezuka Y, Maejima A, Sato T, Nemoto K, Kamioka H, Hakeda Y, and Kumegawa M (1994). Molecular cloning of a possible cysteine proteinase predominantly expressed in osteoclasts. *J Biol Chem* **269,** 1106–1109.

[62] Bromme D, Okamoto K, Wang BB, and Biroc S (1996). Human cathepsin O2, a matrix protein-degrading cysteine protease expressed in osteoclasts. Functional expression of human cathepsin O2 in *Spodoptera frugiperda* and characterization of the enzyme. *J Biol Chem* **271,** 2126–2132.

[63] Bossard MJ, Tomaszek TA, Thompson SK, Amegadzie BY, Hanning CR, Jones C, Kurdyla JT, McNulty DE, Drake FH, Gowen M, and Levy MA (1996). Proteolytic activity of human osteoclast cathepsin K. Expression, purification, activation, and substrate identification. *J Biol Chem* **271,** 12517–12524.

[64] Gelb BD, Shi GP, Chapman HA, and Desnick RJ (1996). Pycnodysostosis, a lysosomal disease caused by cathepsin K deficiency. *Science* **273,** 1236–1238.

[65] Inui T, Ishibashi O, Inaoka T, Origane Y, Kumegawa M, Kokubo T, and Yamamura T (1997). Cathepsin K antisense oligodeoxynucleotide inhibits osteoclastic bone resorption. *J Biol Chem* **272,** 8109–8112.

[66] Hashimoto Y, Kakegawa H, Narita Y, Hachiya Y, Hayakawa T, Kos J, Turk V, and Katunuma N (2001). Significance of cathepsin B accumulation in synovial fluid of rheumatoid arthritis. *Biochem Biophys Res Commun* **283,** 334–339.

[67] Hart CA, Scott LJ, Bagley S, Bryden AA, Clarke NW, and Lang SH (2002). Role of proteolytic enzymes in human prostate bone metastasis formation: *in vivo* and *in vitro* studies. *Br J Cancer* **86,** 1136–1142.

[68] Brubaker KD, Vessella RL, True LD, Thomas R, and Corey E (2003). Cathepsin K mRNA and protein expression in prostate cancer progression. *J Bone Miner Res* **18,** 222–230.

[69] Khan KM and Falcone DJ (1997). Role of laminin in matrix induction of macrophage urokinase-type plasminogen activator and 92-kDa metalloproteinase expression. *J Biol Chem* **272,** 8270–8275.

[70] Bafetti LM, Young TN, Itoh Y, and Stack MS (1998). Intact vitronectin induces matrix metalloproteinase-2 and tissue inhibitor of metalloproteinases-2 expression and enhanced cellular invasion by melanoma cells. *J Biol Chem* **273,** 143–149.

[71] Hornebeck W, Emonard H, Monboisse JC, and Bellon G (2002). Matrix-directed regulation of pericellular proteolysis and tumor progression. *Semin Cancer Biol* **12,** 231–241.

[72] Sappino AP, Busso N, Belin D, and Vassalli JD (1987). Increase of urokinase-type plasminogen activator gene expression in human lung and breast carcinomas. *Cancer Res* **47,** 4043–4046.

[73] Suzumiya J, Hasui Y, Kohga S, Sumiyoshi A, Hashida S, and Ishikawa E (1988). Comparative study of plasminogen activator antigens in colonic carcinomas and adenomas. *Int J Cancer* **42,** 627–632.

[74] Kirchheimer JC, Pfluger H, Ritsch LP, Hienert G, and Binder BR (1985). Plasminogen activator activity in bone metastases of prostatic carcinomas as compared to primary tumors. *Invasion Metastasis* **5,** 344–355.

[75] Sheng S, Pemberton PA, and Sager R (1994). Production, purification, and characterization of recombinant maspin proteins. *J Biol Chem* **269,** 30988–30993.

[76] Cher ML, Biliran HR Jr, Bhagat S, Meng Y, Che M, Lockett J, Abrams J, Fridman R, Zachareas M, and Sheng S (2003). Maspin expression inhibits osteolysis, tumor growth, and angiogenesis in a model of prostate cancer bone metastasis. *Proc Natl Acad Sci USA* **100,** 7847–7852.

[77] Everts V, Delaisse J, Korper W, Niehof A, Vaes G, and Beertsen W (1992). Degradation of collagen in bone-resorbing compartment underlying the osteoclasts involves both cysteine-proteinases and matrix metalloproteinases. *J Cell Physiol* **150,** 221–231.

[78] Tumber A, Papaioannou S, Breckon J, Meikle MC, Reynolds JJ, and Hill PA (2003). The effects of serine proteinase inhibitors on bone resorption *in vitro*. *J Endocrinol* **178,** 437–447.

[79] Eaton CL and Coleman RE (2003). Pathophysiology of bone metastases from prostate cancer and the role of bisphosphonates in treatment. *Cancer Treat Rev* **29,** 189–198.

[80] Teicher BA, Kakeji Y, Ara G, Herbst RS, and Northey D (1997). Prostate

carcinoma response to cytotoxic therapy: *in vivo* resistance. *In Vivo* **11,** 453–461.

[81] Heldin CH, Miyazono K, and ten Dijke P (1997). TGF-beta signalling from cell membrane to nucleus through SMAD proteins. *Nature* **390,** 465–471.

[82] Lindemann RK, Ballschmieter P, Nordheim A, and Dittmer J (2001). Transforming growth factor beta regulates parathyroid hormone–related protein expression in MDA-MB-231 breast cancer cells through a novel Smad/Ets synergism. *J Biol Chem* **276,** 46661–46670.

[83] Yan S, Berquin IM, Troen BR, and Sloane BF (2000). Transcription of human cathepsin B is mediated by Sp1 and Ets family factors in glioma. *DNA Cell Biol* **19,** 79–91.

[84] Delannoy-Courdent A, Mattot V, Fafeur V, Fauquette W, Pollet I, Calmels T, Vercamer C, Boilly B, Vandenbunder B, and Desbiens X (1998). The expression of an Ets1 transcription factor lacking its activation domain decreases uPA proteolytic activity and cell motility, and impairs normal tubulogenesis and cancerous scattering in mammary epithelial cells. *J Cell Sci* **111,** 1521–1534.

[85] Farina AR, Coppa A, Tiberio A, Tacconelli A, Turco A, Colletta G, Gulino A, and Mackay AR (1998). Transforming growth factor-beta1 enhances the invasiveness of human MDA-MB-231 breast cancer cells by up-regulating urokinase activity. *Int J Cancer* **75,** 721–730.

[86] Cataisson C, Gordon J, Roussiere M, Abdalkhani A, Lindemann R, Dittmer J, Foley J, and Bouizar Z (2003). Ets-1 activates parathyroid hormone–related protein gene expression in tumorigenic breast epithelial cells. *Mol Cell Endocrinol* **204,** 155–168.

[87] Naito S, Shimizu S, Matsuu M, Nakashima M, Nakayama T, Yamashita S, and Sekine I (2002). Ets-1 upregulates matrix metalloproteinase-1 expression through extracellular matrix adhesion in vascular endothelial cells. *Biochem Biophys Res Commun* **291,** 130–138.

[88] Thomas GJ, Lewis MP, Hart IR, Marshall JF, and Speight PM (2001). AlphaVbeta6 integrin promotes invasion of squamous carcinoma cells through up-regulation of matrix metalloproteinase-9. *Int J Cancer* **92,** 641–650.

[89] Festuccia C, Angelucci A, Gravina G, Eleuterio E, Vicentini C, and Bologna M (2002). Bombesin-dependent pro-MMP-9 activation in prostatic cancer cells requires beta1 integrin engagement. *Exp Cell Res* **280,** 1–11.

[90] Dalvi N, Thomas GJ, Marshall JF, Morgan M, Bass R, Ellis V, Speight PM, and Whawell SA (2004). Modulation of the urokinase-type plasminogen activator receptor by the beta6 integrin subunit. *Biochem Biophys Res Commun* **317,** 92–99.

[91] Yebra M, Goretzki L, Pfeifer M, and Mueller BM (1999). Urokinase-type plasminogen activator binding to its receptor stimulates tumor cell migration by enhancing integrin-mediated signal transduction. *Exp Cell Res* **250,** 231–240.

[92] Kostenuik PJ, Singh G, and Orr FW (1997). Transforming growth factor beta upregulates the integrin-mediated adhesion of human prostatic carcinoma cells to type I collagen. *Clin Exp Metastasis* **15,** 41–52.

[93] Haywood-Reid PL, Zipf DR, and Springer WR (1997). Quantification of integrin subunits on human prostatic cell lines—comparison of nontumorigenic and tumorigenic lines. *Prostate* **31,** 1–8.

[94] Witkowski CM, Rabinovitz I, Nagle RB, Affinito KS, and Cress AE (1993). Characterization of integrin subunits, cellular adhesion and tumorigenicity of four human prostate cell lines. *J Cancer Res Clin Oncol* **119,** 637–644.

[95] Cooper CR, Chay CH, and Pienta KJ (2002). The role of alpha(v) beta(3) in prostate cancer progression. *Neoplasia* **4,** 191–194.

[96] Hullinger TG, McCauley LK, DeJoode ML, and Somerman MJ (1998). Effect of bone proteins on human prostate cancer cell lines *in vitro*. *Prostate* **36,** 14–22.

[97] Nemeth JA, Cher ML, Zhou Z, Mullins C, Bhagat S, and Trikha M (2003). Inhibition of alpha(v)beta3 integrin reduces angiogenesis, bone turnover, and tumor cell proliferation in experimental prostate cancer bone metastases. *Clin Exp Metastasis* **20,** 413–420.

[98] Rozhin J, Sameni M, Ziegler G, and Sloane BF (1994). Pericellular pH affects distribution and secretion of cathepsin B in malignant cells. *Cancer Res* **54,** 6517–6525.

[99] Tooze J, Hollinshead M, Hensel G, Kern HF, and Hoflack B (1991). Regulated secretion of mature cathepsin B from rat exocrine pancreatic cells. *Eur J Cell Biol* **56,** 187–200.

[100] Wittrant Y, Couillaud S, Theoleyre S, Dunstan C, Heymann D, and Redini F (2002). Osteoprotegerin differentially regulates protease expression in osteoclast cultures. *Biochem Biophys Res Commun* **293,** 38–44.